

Discovery and Structure-Activity Relationship Study of (Z)-5-Methylenethiazolidin-4-one Derivatives as Potent and Selective Pan-phosphatidylinositol 5-Phosphate 4-Kinase Inhibitors

Theresa D. Manz, Sindhu Carmen Sivakumaren, Fleur M. Ferguson, Tinghu Zhang, Adam Yasgar, Hyuk-Soo Seo, Scott B Ficarro, Joseph D Card, Hyeseok Shim, Chandrasekhar V Miduturu, Anton Simeonov, Min Shen, Jarrod A. Marto, Sirano Dhe-Paganon, Matthew D. Hall, Lewis C. Cantley, and Nathanael S Gray

J. Med. Chem., **Just Accepted Manuscript** • DOI: 10.1021/acs.jmedchem.0c00227 • Publication Date (Web): 16 Apr 2020

Downloaded from pubs.acs.org on April 17, 2020

Just Accepted

“Just Accepted” manuscripts have been peer-reviewed and accepted for publication. They are posted online prior to technical editing, formatting for publication and author proofing. The American Chemical Society provides “Just Accepted” as a service to the research community to expedite the dissemination of scientific material as soon as possible after acceptance. “Just Accepted” manuscripts appear in full in PDF format accompanied by an HTML abstract. “Just Accepted” manuscripts have been fully peer reviewed, but should not be considered the official version of record. They are citable by the Digital Object Identifier (DOI®). “Just Accepted” is an optional service offered to authors. Therefore, the “Just Accepted” Web site may not include all articles that will be published in the journal. After a manuscript is technically edited and formatted, it will be removed from the “Just Accepted” Web site and published as an ASAP article. Note that technical editing may introduce minor changes to the manuscript text and/or graphics which could affect content, and all legal disclaimers and ethical guidelines that apply to the journal pertain. ACS cannot be held responsible for errors or consequences arising from the use of information contained in these “Just Accepted” manuscripts.

1
2
3
4
5
6
7
8
9
10
11
12
13
14
15
16
17
18
19
20
21
22
23
24
25
26
27
28
29
30
31
32
33
34
35
36
37
38
39
40
41
42
43
44
45
46
47
48
49
50
51
52
53
54
55
56
57
58
59
60



SCHOLARONE™
Manuscripts

Discovery and Structure-Activity Relationship Study of (Z)-5-Methylenethiazolidin-4-one Derivatives as Potent and Selective Pan-phosphatidylinositol 5-Phosphate 4-Kinase Inhibitors

Theresa D. Manz,^{†,‡,⊥,°} Sindhu Carmen Sivakumaren,^{†,‡,°} Fleur M. Ferguson,^{†,‡} Tinghu Zhang,^{†,‡} Adam Yasgar,^Δ Hyuk-Soo Seo,^{†,‡} Scott B. Ficarro,^{ψ,Θ,φ} Joseph D. Card,^{ψ,Θ,φ} Hyeseok Shim,[§] Chandrasekhar V. Miduturu,^{†,‡} Anton Simeonov,^Δ Min Shen,^Δ Jarrod A. Marto,^{ψ,Θ,φ} Sirano Dhe-Paganon,^{†,‡} Matthew D. Hall,^Δ Lewis C. Cantley,[§] and Nathanael S. Gray^{†,‡,*}

[†]Department of Cancer Biology, Dana-Farber Cancer Institute, 360 Longwood Avenue, Boston, MA 02215, USA

[‡]Department of Biological Chemistry and Molecular Pharmacology, Harvard Medical School, Boston, MA 02215, USA

[⊥]Department of Pharmaceutical and Medicinal Chemistry, Saarland University, 66123 Saarbruecken, Germany

^ΔNational Center for Advancing Translational Sciences, National Institutes of Health, Rockville, MD, USA

^ψDepartment of Cancer Biology and Blais Proteomics Center, Dana-Farber Cancer Institute, Boston, MA 02215, USA

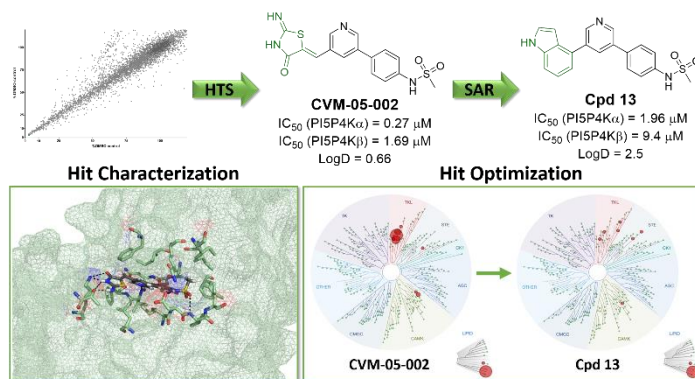
^ΘDepartment of Oncologic Pathology, Dana-Farber Cancer Institute, 360 Longwood Avenue, Boston, MA 02215, USA

^φDepartment of Pathology, Brigham and Women's Hospital, Harvard Medical School, Boston, MA 02215, USA

[§]Meyer Cancer Center, Weill Cornell Medicine and New York Presbyterian Hospital, New York, NY 10065, USA

[°]These authors contributed equally to this work.

ABSTRACT: Due to their role in many important signaling pathways, phosphatidylinositol 5-phosphate 4-kinases (PI5P4Ks) are attractive targets for the development of experimental therapeutics for cancer, metabolic and immunological disorders. Recent efforts to develop small molecule inhibitors for these lipid kinases resulted in compounds with low- to sub-micromolar potencies. Here, we report the identification of CVM-05-002 using a high-throughput screen of PI5P4K α against our in-house kinase inhibitor library. CVM-05-002 is a potent and selective inhibitor of PI5P4Ks and a 1.7 Å X-ray structure reveals its binding interactions in the ATP-binding pocket. Further investigation of the structure-activity relationship led to the development of compound **13**, replacing the rhodanine-like moiety present in CVM-05-002 with an indole, a potent pan-PI5P4K inhibitor with excellent kinome-wide selectivity. Finally, we employed isothermal cellular thermal shift assays (CETSA) to demonstrate effective cellular target engagement of PI5P4K α and - β by the inhibitors in HEK 293T cells.



KEYWORDS: drug discovery, lipid kinase inhibitors, PI5P4K, structure-activity relationship, cellular thermal shift assay, phosphoinositide

INTRODUCTION

Phosphoinositides, such as phosphatidylinositol-4,5-bisphosphate (PI-4,5-P₂), are key players in many cell-regulating and -signaling processes. Inositide function is controlled by lipid kinases, which alter their phosphorylation pattern, thus generating a range of signaling molecules with different downstream effects. Phosphatidylinositol 5-phosphate 4-kinases (PI5P4Ks) represent a family of these lipid kinases, that have been shown to phosphorylate phosphatidylinositol 5-phosphate (PI5P) on its 4-position to produce PI-4,5-P₂.¹ In healthy cells, PI5P4Ks play

a role in regulating cellular metabolism, stress response, and immunological processes,²⁻⁷ while abnormal function of these lipid kinases has been linked to diseases, such as diabetes and cancer.⁸⁻¹¹ As a result, PI5P4K inhibitors pose potentially important therapeutic agents, for example, in oncology. To date, several small molecule PI5P4K inhibitors with low- or sub-micromolar potency have been reported in the literature,¹²⁻¹⁷ including our recently reported phenylamino pyrimidine-based, covalent pan-PI5P4K inhibitors, THZ-P1-2 and compound **32** (labeled compound “**30**” in the original publication; Supporting Figure 1).^{16,17}

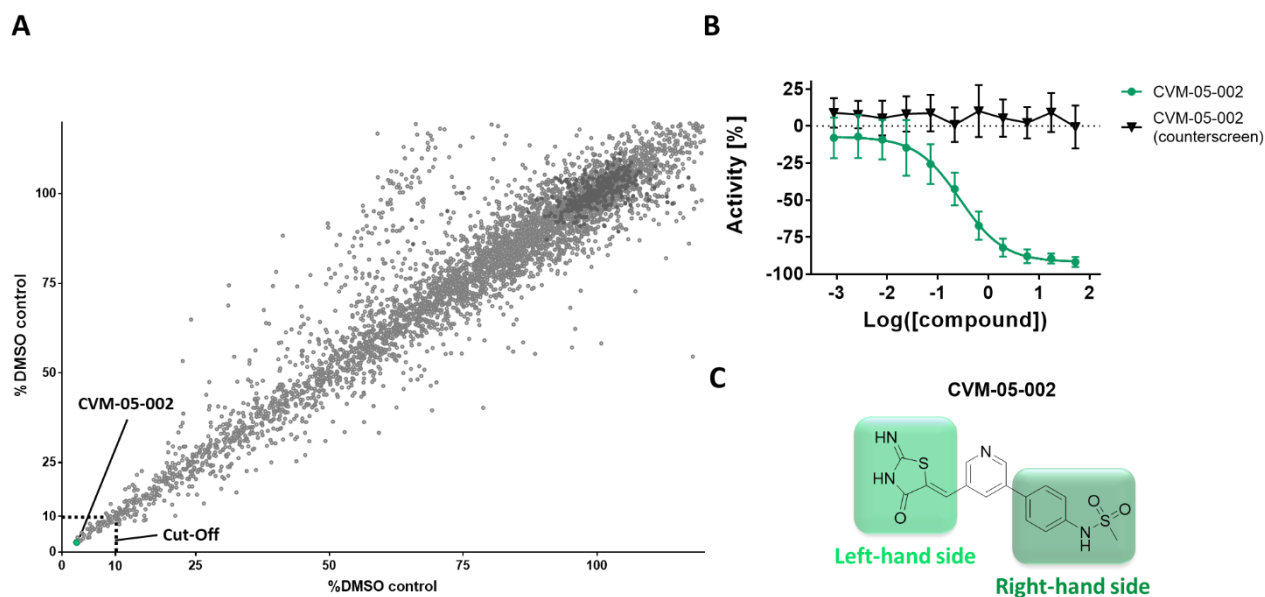


Figure 1. **A.** Scatter plot of high-throughput screen for PI5P4K α activity of in-house small molecule library with ~6,000 compounds (shown are hits at <120% DMSO control). The results of two replicates are plotted against each other (normalized to DMSO). Negative controls (DMSO) are shown in dark gray, CVM-05-002 is depicted in green, and the 10% DMSO control cut-off (90% inhibition) is labeled. **B.** Concentration-response curves of CVM-05-002 including counterscreen results. **C.** Structure of identified lead compound, CVM-05-002.

Here we report our efforts to find chemically distinct PI5P4K inhibitors, that can serve as chemical probes for further drug development efforts. We focused on developing reversible inhibitors, that would not be susceptible to potentially acquired resistance through mutation of the active site cysteine residue, which is modified by irreversible PI5P4K inhibitors.^{16,17} A prominent example of this type of resistance mechanism is the EGFR C797S mutation that develops in non-small cell lung cancer following treatment with irreversible small molecule EGFR inhibitor AZD9291, and renders tumors resistant.¹⁸

In order to find novel, reversible PI5P4K inhibitor scaffolds, we performed a high-throughput screen of our internal kinase inhibitor library, containing approximately 6,000 structurally diverse compounds developed and synthesized in our lab against PI5P4K α , using an ADP-Glo assay to measure PI5P4K α kinase activity. This screen identified potent hit compound CVM-05-002 (IC₅₀ 270 nM). CVM-05-002 contains a distinct (Z)-5-methylenethiazolidin-4-one moiety, which can be described as a rhodanine-like structure. Although rhodanine-type compounds can function as pan-assay interference compounds (PAINS) in AlphaScreen assays,¹⁹⁻²² in other settings, rhodanines and their derivatives elaborated through focused medicinal chemistry campaigns²³⁻²⁶ have been advanced into clinical trials.²⁷ In this study, we describe the discovery, validation and structure-activity relationship (SAR) of compounds based on this scaffold as potent, specific pan-PI5P4K inhibitors.

RESULTS AND DISCUSSION

High-Throughput Screen. Since reliable ADP-Glo-based assays for PI5P4K α inhibition have been previously described,¹² we adapted this assay to establish a protocol for a miniaturized high-throughput screen. We optimized the assay to perform in a 384-well format with respect to PI5P4K α enzyme concentration and ADP-Glo reagent volumes to obtain a robust signal-to-background ratio, a stable Z'-factor (0.85), and a low coefficient of variation (CV = 0.098) (Supporting Figure

2). Our in-house compound library, consisting of diverse kinase inhibitor scaffolds, was screened at a concentration of 66 μ M. This relatively high concentration was chosen based on previous reports describing low potency inhibition of PI5P4K by known kinase inhibitor scaffolds, indicating that identification of a highly potent inhibitor for this subfamily of lipid kinases maybe more challenging than for the protein kinase family. Our screen resulted in the identification of approximately 50 hits exhibiting > 90% inhibition (Figure 1A, Supporting Figure 3 and 4). With a mean of 2.7% DMSO control, CVM-05-002 showed the strongest effects in the screen. All identified hits were analyzed regarding diversity of the scaffolds, and historical data relating to kinase selectivity was examined. Highly promiscuous or potentially covalent scaffolds were excluded from the set. Based on this, a subset of hit compounds was tested in an 11-point concentration-response experiment, which confirmed CVM-05-002 as the most potent hit for PI5P4K α inhibitory activity (IC₅₀ 0.27 μ M, Figure 1B, C). We verified that the PI5P4K α activity was not due to compound interactions with assay reagents. This was done by counterscreening at a fixed ADP/ATP concentration ratio representing 20% conversion but excluding the PI5P4K α enzyme as well as the lipid substrate, confirming no assay interference with CVM-05-002 (Figure 1B).

Interestingly, several structurally similar molecules to CVM-05-002 were present in the library, while only four analogs were found among the top hits identified in the high-throughput screen. Subsequent testing of these hits in our ADP-Glo-based PI5P4K α assay revealed that those analogs are ~30-fold less potent than CVM-05-002, or more (data not shown). Furthermore, closest analogs of CVM-05-002, only differing in the 3,5-substituted pyridine moiety of the hit compound, showed strong PIM kinase off-targets (Supporting Table 1). This was not surprising, since similar scaffolds have been shown to be potent PIM kinase inhibitors.²⁶ However, since CVM-05-002 was the only compound of this scaffold without any PIM kinase off-

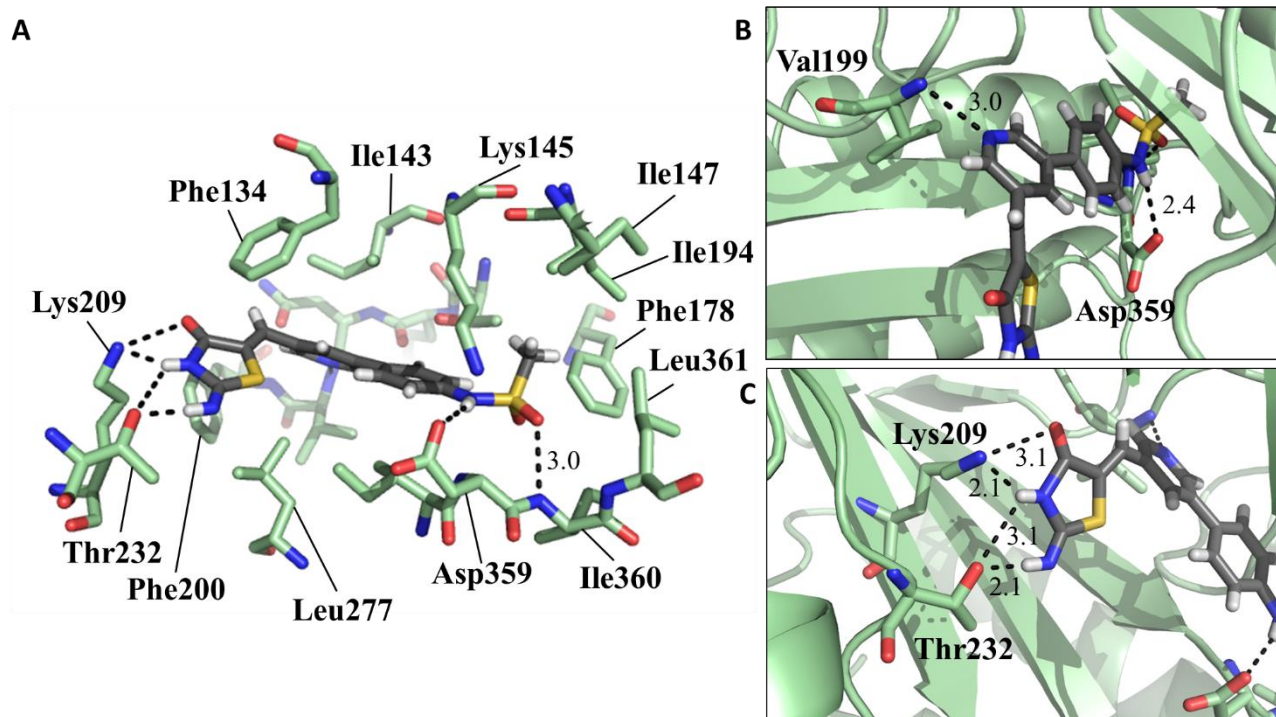


Figure 2. A. Binding site of co-crystal structure of PI5P4K α with bound inhibitor CVM-05-002 (dark gray). Key hydrogen bond interactions are depicted by dashed lines (numbers indicate distances in Å). B. Key hydrogen bond interactions of the hinge-binding site are shown as dashed lines (numbers indicate distances in Å). C. Proposed hydrogen bond network of the thiazolidinone moiety of CVM-05-002 with Lys209 and Thr232 (interactions shown as dashed lines; numbers indicate distances in Å). PDB-ID: 6UX9.

target activity, carrying a unique 3,5-substituted pyridine moiety, while showing potent on-target activity, we were highly motivated to further optimize this screening hit and explore its SAR.

Finally, knowing that the scaffold of CVM-05-002 could potentially have nonspecific effects due to its similarity to compounds with reported reactivity,²² we performed mass spectrometry analysis of recombinant PI5P4K α and - β , incubated with CVM-05-002. PI5P4K α showed no detectable reaction after 2 hours, while the β -isoform of the lipid kinase was modified only at a very low level (~14%). Under the same conditions, our previously reported covalent PI5P4K inhibitor, THZ-P1-2,¹⁷ labeled ~63-87% of both isoforms (Supporting Figures 5 and 6).

Structural Basis of the CVM-PI5P4K Interaction. Recombinant PI5P4K α was co-crystallized in complex with CVM-05-002 at 1.7 Å resolution, confirming a non-covalent binding mode of the inhibitor in the active site of the lipid kinase (Figure 2) (PDB-ID: 6UX9).

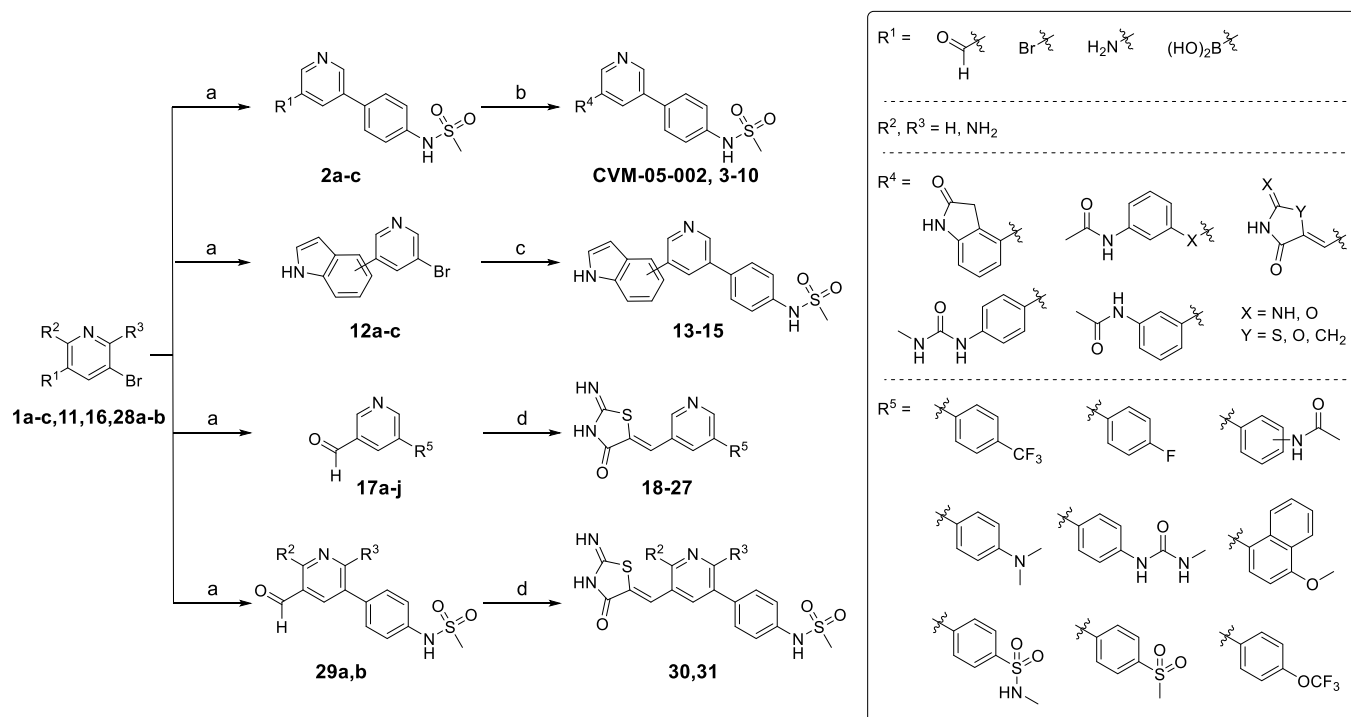
The obtained co-crystal structure revealed general hydrophobic interactions of CVM-05-002 with the ATP-binding pocket. For example, Phe178, Ile147, Ile194, and Leu361 form a non-polar pocket encasing the methyl group of the sulfonamide (Figure 2A). In addition, five key hydrogen bonding interactions could be identified. At the hinge, the pyridine nitrogen anchors the inhibitor *via* a hydrogen bond with the backbone of Val199 (Figure 2B). The thiazolidinone moiety interacts with the side chains of Thr232 and Lys209 on the left-hand side of the scaffold, while the sulfonamide engages in two hydrogen bonding interactions with the backbone of Ile360 and the sidechain of Asp359 on the right-hand side (Figure 2A). Furthermore, Asp359 and Lys145 form a salt-bridge, potentially improving the hydrogen bonding interaction with the sulfonamide-NH.

Likewise it should be noted, that the thiazolidinone moiety is positioned in a way, that permits formation of hydrogen bonding interactions of the imine, the carbonyl, and the cyclic-NH group with Thr232 and Lys209, together forming a fork-like hydrogen bond network of the left-hand side of the inhibitor with the binding site. While the interaction of the pyridine moiety seemed to be essential for the selectivity of the molecule (Supporting Figure 1), the strong left- and right-hand side hydrogen bond interactions are likely contributing to the relatively high potency of this scaffold (Figure 2A and 2C).

Selectivity Screening. The kinome-wide binding selectivity of CVM-05-002 at 1 μ M concentration was determined, using the commercial KINOMEscan profiling platform, consisting of 468 kinases. CVM-05-002 showed an excellent selectivity profile (Figure 3; selectivity score for hits with percent control < 35, $S_{35} = 0.02$), providing further evidence that this inhibitor is a selective and potent pan-PI5P4K inhibitor. Taken together, these findings were encouraging to pursue further medicinal chemistry efforts to better understand the SAR around this promising hit.

Chemistry. Given the above, the presented SAR study focuses mainly on changes regarding the thiazolidinone and the *N*-phenylmethanesulfonamide groups, decorating the hinge-binding pyridine moiety and being referred to as left- and right-hand side of the scaffold, respectively (Figure 1C). Hence, two main series of CVM-05-002 analogs were designed as summarized in Tables 1 and 2, with changes made on either side of the molecule.

In general, CVM-05-002 and analogs were synthesized as summarized in Scheme 1, starting from a 3-bromopyridine analog (**1**, **11**, **16**, **28a-b**) and by introducing different aromatic ring systems *via* Suzuki couplings (**2a-c**, **6-8**, **12a-c**, **13-15**,

Scheme 1. Synthesis of Compound CVM-05-002 and Analogs^a

^a Reagents and Conditions: (a) Phenylboronic acids/respective pinacol boronic acid esters, Pd(PPh₃)₂Cl₂, Cs₂CO₃, 1,4-dioxane/H₂O, 100 °C, 1.5 h, 9-93% yield; (b) (Z)-methylenethiazolidinone derivative, β-alanine, AcOH, 100 °C, 0.5 h, 12-33% yield, or maleimide, PPh₃, DCM, rt, overnight, 21% yield, or oxazolidine-2,4-dione, piperidine, EtOH, 100 °C, overnight, 4% yield, or phenylboronic acids/respective pinacol boronic acid ester, Pd(PPh₃)₂Cl₂, Cs₂CO₃, 1,4-dioxane/H₂O, 100 °C, 1.5 h, 1-37% yield, or N-(3-hydroxyphenyl)acetamide, CuI, K₂CO₃, DMF, 120 °C, 2 d, 3% yield, or N-(3-bromophenyl)acetamide, Pd₂(dba)₃, X-Phos, K₂CO₃, 1,4-dioxane/H₂O, 80 °C, overnight, 7% yield; (c) 4-(methanesulfonylamino)phenylboronic acid pinacol ester, Pd(PPh₃)₂Cl₂, Cs₂CO₃, 1,4-dioxane/H₂O, 100 °C, 1.5 h, 19-27% yield; (d) 2-iminothiazolidin-4-one, β-alanine, AcOH, 100 °C, 0.5 h, 4-22% yield.

17a-j, and **29a,b**). (Z)-methylenethiazolidinone and its analogs were accessed from nicotinaldehyde derivatives, which were coupled with either 2-iminothiazolidin-4-one, oxazolidine-2,4-dione, or maleimide, using different Knoevenagel condensation reaction conditions (CVM-05-002, **3-5**, **18-27**, and **30-31**). Compounds **9** and **10** were yielded *via* S_N2 reactions with different 3-substituted N-phenylacetamide analogs.

Biological Evaluation. The biochemical inhibition of PI5P4Kα and -β was determined as previously described.^{12,17} Due to its low enzymatic activity,^{28,29} we were unable to determine PI5P4Kγ activity for our compounds, thus, this discussion focuses solely on the PI5P4Kα and -β isoforms. It should be noted, that structure alignment of all three PI5P4Ks confirmed that the binding pocket is highly conserved within this lipid kinase family (Supporting Figure 7). The amino acids, highlighted in Figure 2 are identical among all three isoforms, with the exception of Ile147 and Ile194 in PI5P4Kα, which are being replaced by valines in PI5P4Kβ or a valine and a leucine, respectively, in PI5P4Kγ. Val199 in PI5P4Kα is a methionine in PI5P4Kγ, which should not affect the hinge binding of CVM-05-002, since the interaction of the pyridine is with the backbone of the amino acid.

In this biochemical evaluation, our initial hit compound, CVM-05-002, showed consistent IC₅₀ values of 270 nM and 1.69 μM for PI5P4Kα and -β, respectively, hence, representing – to the best of our knowledge – the most potent reported pan-PI5P4K inhibitor to date. However, CVM-05-002 is a polar compound with a LogD value of 0.66, which limits its use in

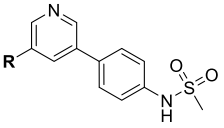
cells and, subsequently, as a useful probe to study PI5P4Ks *in vivo*. The balance of lipophilicity and PI5P4K inhibitory activity was therefore another crucial criterium of this SAR study.

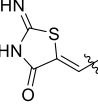
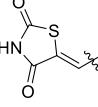
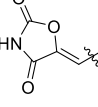
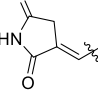
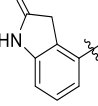
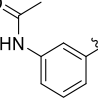
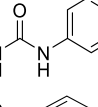
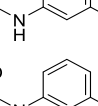
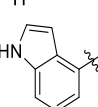
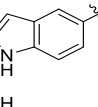
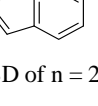
With a first set of compounds, summarized in Table 1, we introduced different substituents to the left-hand side of the scaffold, altering or replacing the methylenethiazolidinone moiety. For example, changing the imine of the thiazolidinone to a carbonyl (compound **3**) slightly improved inhibitory activity with respect to PI5P4Kα by about 2-fold to an IC₅₀ of 133 nM, while the β-activity did not change. This is not surprising, since the carbonyl-O and the imine-NH can both function as hydrogen bond acceptors. However, an oxazolidine-2,4-dione in compound **4** led to an inactive compound on both isoforms, highlighting the importance of the electro-chemical properties of this five-membered ring system for PI5P4K activity, since the electronegativity of oxygen (compound **4**) is much higher as compared to sulfur (compound **3**). This is further supported by the fact that introducing a carbon (compound **5**) – having similar electronegativity as sulfur – in position of the oxygen (compound **4**) led to a moderately active compound with IC₅₀s of 6.1 and 27 μM for PI5P4Kα and -β, respectively. It should be noted, that this equals a 1-2-log-fold drop in PI5P4K activity of compound **5** compared to compound **3**, pointing towards an essential role of the cyclic sulfur for the PI5P4K activity of the scaffold. One major difference between the five membered ring systems of compounds **3** and **5** is the aromaticity. Whereas compound **3** shows aromatic features due to the lone electron pairs

of the sulfur, compound **5** introduces a sp^3 -hybridized carbon atom, disrupting the aromatic π -system of the ring.

All compounds mentioned above have lower LogD values than CVM-05-002, with compound **3** and **5** having a LogD of

Table 1. IC₅₀ Evaluation of Compound CVM-05-002, 3-15



Cpd	R	IC ₅₀ [μ M] ^a				LogD
		PI5P4K				
		$-\alpha$	n	$-\beta$	n	
CVM-05-002		0.27 \pm 0.035	3	1.7 \pm 0.50	3	0.66
3		0.13 \pm 0.032	3	1.9 \pm 0.42	3	-0.05
4		21 \pm 1.4	3	>50	2	-1.0
5		6.1 \pm 0.0	3	27 \pm 13	2	-0.14
6		8.9 \pm 2.9	3	15 \pm 9.0	3	1.5
7		5.3 \pm 0.72	3	36 \pm 4.1	3	1.7
8		3.7 \pm 0.24	3	43 \pm 21	2	1.6
9		9.0 \pm 0.61	3	25 \pm 8.9	3	1.5
10		14 \pm 0.96	3	45 \pm 28	2	1.5
13		2.0 \pm 0.45	3	9.4 \pm 7.1	2	2.5
14		2.1 \pm 0.53	3	22 \pm 8.4	2	2.5
15		3.2 \pm 0.21	3	29 \pm 4.1	2	2.5

^a Average \pm SD of n = 2 or n = 3 experiments, each using an 11-point titration.

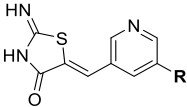
around 0, while compound **4** has the lowest LogD value of the set with -1. Consequently, we next focused on replacing the entire methylenethiazolidinone moiety to improve lipophilicity of the inhibitors. Strategies for this replacement were inspired by the co-crystal structure, which suggests that the (Z)-5-methylenethiazolidin-4-one could be cyclized, by linking the methylene-H with the cyclic carbonyl to form an aromatic six-membered ring. An initial version of this is compound **6**, carrying an indolinone moiety at the left-hand side. This structure is closely related to compound **5**, since the five-membered ring systems of both compounds only differ in the carbonyl oxygen in the 2-position, which is missing in compound **6**. Here, an aromatic six-membered ring, directly connecting to the pyridine, was introduced instead. The compound showed IC₅₀s of 8.9 and 15 μ M for PI5P4K α and $-\beta$, respectively, which is comparable to compound **5**'s PI5P4K activity, while improving LogD by 1.5-log-folds to 1.5. Interestingly, the loss of the carbonyl interaction did not seem to affect the overall PI5P4K activity, which might indicate a positive effect of the aromatic six-membered ring system of compound **6** for PI5P4K activity, potentially compensating for the loss of the carbonyl hydrogen bond interaction.

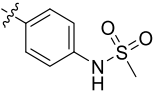
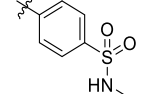
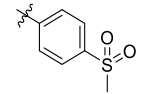
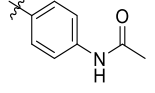
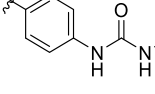
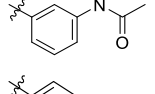
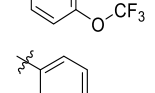
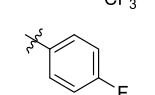
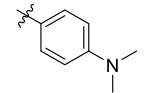
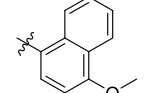
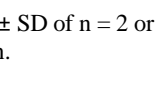
Due to the overall connected π -electron-system in compound **6**, the molecule is likely rather flat, as compared to CVM-05-002, which shows a slight bend at the methylene linker between pyridine and thiazolidinone moiety in the co-crystal structure (Figure 2). Thus, left-hand side residues with higher flexibility, especially in the hydrogen bond forming groups to compensate for this were of interest to us. Ring opening of the pyrrolidine-2-one ring, resulting in a more flexible amid in compound **7**, led to minor improvements in PI5P4K α activity, while showing a slight drop in $-\beta$ activity with IC₅₀s of 5.3 and 36 μ M, respectively. This trend was further pronounced in compound **8**, introducing a methylated urea motif in para-position of the aromatic ring system, with IC₅₀s of 3.7 μ M for PI5P4K α and 43 μ M for PI5P4K β . Compound **8** offers more potential hydrogen bond interactions than the acetamide of compound **7**, which could be an explanation for its slightly higher potency on the α -isoform of the lipid kinase. It should be noted, however, that even though there seems to be a drop in PI5P4K β activity of over 2-fold from compound **6** to compound **8**, that the relatively high standard deviation values are causing the differences in IC₅₀ values to be statistically non-significant.

Introduction of an O- or NH-linker to compound **7** (compounds **9** and **10**, respectively) are further increasing the flexibility of the acetamide to form hydrogen bond interactions with the lipid kinase. Both compounds showed a slight loss in PI5P4K α activity by about 2-3-fold compared to compound **7**, while there was no significant difference in PI5P4K β activity. In summary, comparing the overall lipophilic efficiency (LipE) of these molecules, the flatness of the SAR for compounds **6** to **10** becomes obvious. LipE is an important feature in drug discovery, since it sets the lipophilicity of a molecule in relation to its activity – here, LogD to pIC₅₀. Since compounds **6** to **10** have very similar LogD values, plotting against pIC₅₀ shows that the compounds depict almost identical PI5P4K α and $-\beta$ activity profiles with LipE values between 3 and 4 for PI5P4K α and of values of about 3 for PI5P4K β (Supporting Figure 10), clearly showing no real improvement of PI5P4K activity by more flexible hydrogen bond offering moieties. These findings indicate a limited benefit of the hydrogen bond interactions in Figure 2C, while highlighting the gained PI5P4K activity through the introduced aromatic ring system.

When further simplifying the bicycle of compound **6** by introducing an indole at the left-hand side of the molecule (compound **13**), activity on both PI5P4K isoforms could be improved to low micromolar IC₅₀s. While the slight improvement on PI5P4K β activity is not significant, PI5P4K α activity of compound **13** improves significantly to 2.0 μ M (P value = 0.049 by *t*-test) as compared to compound **6**. This further supports our findings, that the aromaticity of the bicyclic system is more important than the hydrogen bonding interaction by the lactam. Hence, removing the carbonyl of compound **6**, while increasing the aromaticity across both rings of the bicyclic moiety, did not

Table 2. IC₅₀ Evaluation of Compounds 18-27



Cpd	R	IC ₅₀ [μ M] ^a				LogD
		PI5P4K				
		$-\alpha$	n	$-\beta$	n	
CVM-05-002		0.27		1.7		0.66
		\pm	3	\pm	3	
18		1.4		4.3		1.1
		\pm	3	\pm 1.1	2	
19		35		>50		1.1
		\pm 57	3		2	
20		11		>50		1.5
		\pm 4.2	3		3	
21		1.8		8.6		1.4
		\pm	3	\pm 1.9	2	
22		11		>50		1.5
		\pm	3		3	
23		11		>50		3.7
		\pm 5.2	3		2	
24		>50		26		3.2
			3	\pm 3.3	3	
25		>50		28		2.4
			3	\pm 3.2	3	
26		8.8		>50		2.4
		\pm 5.8	3		2	
27		3.9		>50		3.1
		\pm	3		2	
		0.82				

^a Average \pm SD of n = 2 or n = 3 experiments, each using an 11-point titration.

result in loss in potency of the compound, but actually improved the potency on PI5P4K α . Consequently, the higher lipophilicity with a LogD value of 2.5, which is an improvement of over 1-log-fold as compared to compounds **6** to **10**, as well as the enlarged aromatic ring system of compound **13** are beneficial for PI5P4K α activity, but also likely improve properties of the compound for the use in cells.

We assume that this benefit of aromatic moieties at the left-hand side could be indicating π - π -interactions with either Phe200 or Phe134 (Figure 2A), which we had previously identified as a crucial interaction for our reported covalent pan-PI5P4K inhibitor series.¹⁷ This was supported by the fact that further changes in the attachment site of the indole from the 4-position (compound **13**) to the 5- or 6- position (compounds **14** and **15**, respectively) led to no change in PI5P4K α activity, and only a minor 2-3-fold decrease in β -activity. Even though compounds **13-15** show, thus, a very similar PI5P4K activity profile, compound **13** – the isomer closely related to compound **6** – showed the best combined PI5P4K α and $-\beta$ activity. As already mentioned, since all three compounds have improved LogD values of 2.5, leading to LipE values of around 3 for PI5P4K α and values of 2-2.5 for PI5P4K β , the compounds should show good cellular target engagement, considering the improved balance of lipophilicity and biochemical activity as compared to the initial hit compound, CVM-05-002 (Supporting Figure 10A and 10B).

In a next step, the SAR of the right-hand side of CVM-05-002 was investigated by introducing aromatic ring systems, carrying different substituents ranging from polar sulfonamides, amides and urea motifs to non-polar and bulkier moieties (Table 2). The sulfonamide moiety in CVM-05-002 significantly contributes to the compound's high hydrophilicity, which inspired designs that aim to create compounds of higher lipophilicity, while at the same time interrogating the necessity of the sulfonamide of the parent compound for PI5P4K activity.

Compound **18**, a reversed sulfonamide analog of CVM-05-002, lost activity against both PI5P4K isoforms by about 1-log-fold, most likely due to the changed hydrogen bond donor/acceptor configuration. Removing the sulfonamide-NH in compound **19** kept the LogD of the compound comparable to compound **18** at 1.1, however, the overall polar surface area (PSA) of the compound decreased from 112 for CVM-05-002 and compound **18** to 100 for compound **19**. Interestingly, losing this additional NH hydrogen bonding interaction led to complete loss of activity on PI5P4Ks. These results might indicate, that the sulfonamide moiety of CVM-05-002 is crucial for optimal PI5P4K activity.

Switching from a sulfonamide to an acetamide (compound **20**) increased lipophilicity by about 1-log-fold, compared to CVM-05-002, to a LogD value of 1.5. Nevertheless, the trigonal-planar conformation of the amide, in contrast to the tetrahedral conformation of the sulfonamide, led to an activity decrease of 2-log-folds or higher on the PI5P4K isoforms. The configuration of the amide in compound **20** makes it impossible for the hydrogen of the NH and the oxygen-O to point into the same direction, which is necessary to form both hydrogen bond interactions seen for CVM-05-002 with Asp359 and Ile360. This is further supported by compound **21**, carrying a methylated urea motif and showing improved biochemical potency on both PI5P4K isoforms to levels comparable to the reversed sulfonamide analog **18**, while having a higher LogD of around 1.4. The additional NH-moiety in compound **21** is likely forming

similar interactions to the NH-group of compound **18**, which would explain the similar potency, as well as the lack in potency of compound **20**. Changing the acetamide from *p*- to *m*-position (compound **22**) did not influence PI5P4K activity, underlining a certain tolerance in this substituent. The meta-position could either point towards the deeper pocket, or towards the thiazolidinone moiety, which would mean that both, the NH or the carbonyl-O could potentially form hydrogen bond interaction with Asp359 or Ile360.

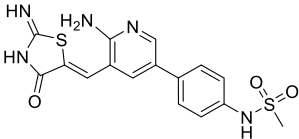
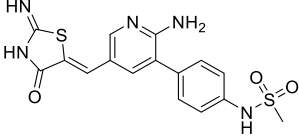
Interestingly, compound **23**, carrying a trifluoromethoxy substituent, exhibited the same activity profile as compound **20** with weak PI5P4K α (11 μ M) and no PI5P4K β activity. This points towards a tolerance for hydrogen bond donors as well as acceptors for PI5P4K α in this position, which is in accordance with the co-crystal structure, since Lys145 is in reach to form hydrogen bond interactions with the methoxy-O (2.4 Å). Removing the hydrogen bond acceptor, resulting in compound **24**, supports this hypothesis by showing loss of PI5P4K α activity. In addition to that, compounds **23** and **24** exhibit good lipophilicity for cellular treatments with LogD values of 3.7 and 3.2, respectively, while the matched methoxy or methyl substituents would have had LogD values of only 1.4 or 1.9 instead. Surprisingly, compound **24** gained back some PI5P4K β activity with an IC₅₀ of 26 μ M. However, this β -activity does not seem to be influenced by the trifluoromethyl moiety, since a simple fluoro substituent (compound **25**) led to the same activity profile. Furthermore, comparing compounds **23** and **25**, it seems that the polar NH- or O-groups adjacent to the aromatic ring are beneficial for PI5P4K α activity, whereas unfavorable in the context of PI5P4K β activity, which is in contrast to the high similarity of the two binding sites (Supporting Figure 7).

Similarly, compounds **26** and **27** introduce either a dimethylamine or a methoxy group, respectively, in para-position of the phenyl moiety at the right-hand side. These substituents pose hydrogen bond acceptors, leading to the activity pattern already seen above with PI5P4K α , but no β -activity. Interestingly, the bulky naphthalene of compound **27** was well tolerated by PI5P4K α and even led to a slight increase in IC₅₀ (3.9 μ M) as compared to compound **23** (11 μ M). Despite the desirable lipophilicity of these two molecules with LogD values of 2.4 and 3.1 for compounds **26** and **27**, respectively, the lack of PI5P4K β activity, as seen with other compounds of this batch of CVM-05-002 analogs, makes them unfit as pan-PI5P4K inhibitor probes. Taken together, it appears that trying to increase lipophilicity by changing the right-hand side of the molecule led to either poor PI5P4K α or β inhibitors, while even slight changes in the sulfonamide moiety of CVM-05-002 led to a drop in PI5P4K activity of at least 1-log-fold. These findings suggest that the sulfonamide of CVM-05-002 is indeed necessary to maintain both PI5P4K α and β activity.

In summary, the SAR analysis of left- and right-hand sides of the PI5P4K inhibitor scaffold revealed that the key interactions seen in the co-crystal structure of PI5P4K α with CVM-05-002 seem to be essential for the potency of the inhibitor. Removal of hydrogen bond donors or acceptors on either side of the molecule generally led to a minimum of 1-log-fold decrease in potency. Interestingly, replacing the (*Z*)-methylenethiazolidinone moiety with an aromatic bicyclic indole (compound **13**) retained good potency comparable to our previously reported pan-PI5P4K inhibitors (Supporting Figure 1),¹⁷ while improving the lipophilicity of the scaffold by about 2-log-folds.

Although we had shown that the 3,5-substituted pyridine is likely essential for the CVM-05-002's kinome-wide selectivity (Supporting Table 1), we had noticed a small pocket extending from the 2-position of the pyridine at the hinge-binding region (Supporting Figure 8). Hence, we designed and synthesized the additional compounds **30** and **31** with an amino group at either the 2- or 6-position of the central pyridine of CVM-05-002. According to the co-crystal structure, the amino group of compound **30** should cause a steric clash with the protein surface at the hinge, whereas compound **31** should be able to fit the amino group into the adjacent pocket, potentially causing a shift in the compound's selectivity profile. The polar amino group was chosen, since the backbone carbonyl of Arg197 as well as the side chain hydroxyl group of Thr196 are in close proximity to the pyridine with distances under 4 Å (Supporting Figure 8). 2-Aminopyridine moieties are also well-known hinge-binding motifs of kinase inhibitors, since they mimic the adenine binding interactions of ATP.³⁰⁻³² As expected, compound **30** lost activity on both, PI5P4K α and β , by almost 1.5-log-folds with IC₅₀s of 4.0 and 25 μ M, respectively (Table 3). In contrast to this 15-fold decrease in potency, compound **31** showed only a very minor decrease in potency with 660 nM and 2.7 μ M potency on PI5P4K α and β , respectively. Naturally, both compounds are more polar than the parent inhibitor, CVM-05-002, with LogD values of 0.4.

Table 3. IC₅₀ Evaluation of Compounds 30, 31

Cpd	Structure	IC ₅₀ [μ M] ^a		Log D
		PI5P4K - α	- β	
30		4.0	25	0.41
		± 0.73	± 2.9	
31		0.66	2.7	0.41
		± 0.040	± 0.17	

^a Average \pm SD of three experiments, each using an 11-point titration.

Selectivity Profiling. Selected compounds of our series were tested on a set of 468 kinases in Ambit's commercially available KINOMEScan platform. Besides our most potent pan-PI5P4K inhibitors (CVM-05-002, as well as compounds **3** and **31**), compound **13**, with the best balance between lipophilicity and biochemical activity, was selected as well. The compounds' binding activity was determined at 1 μ M as percent DMSO control and is summarized in Figure 3. It should be noted, that PI5P4K α was not available in this profiling panel.

Our initial hit compound, CVM-05-002 (selectivity score for hits with percent control < 35; S₃₅ = 0.02), showed high selectivity among the kinases tested, with only 10 hits at a cut-off of 35 % DMSO control, such as ACVR2A and TGFBR2, both of which are members of the TGF β family receptors.³³⁻³⁵ Within the lipid kinases, PI5P4K γ is the only strongly bound target, suggesting excellent selectivity of the inhibitor within the lipid kinase families. PI5P4K β did not show up as a hit in this assay,

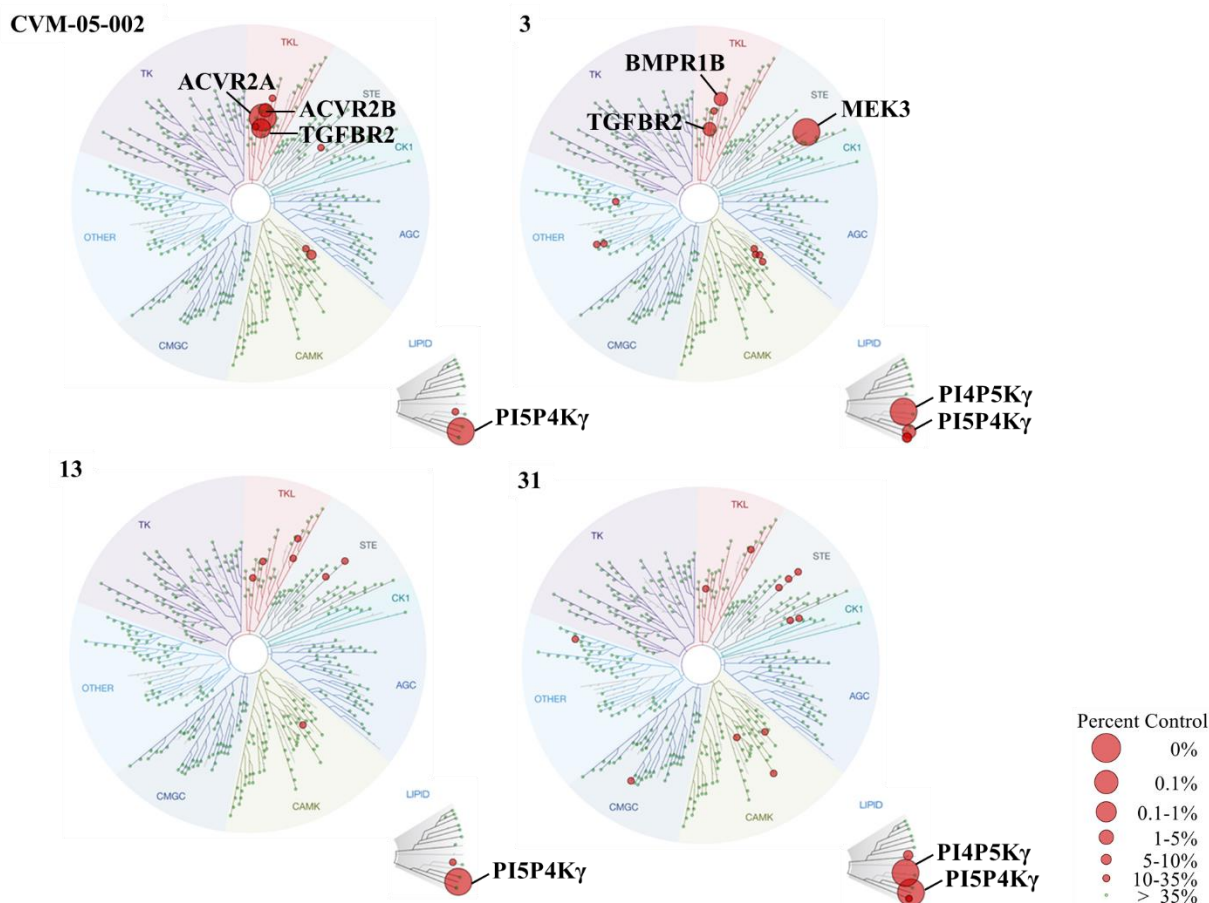


Figure 3. Kinome-wide selectivity profile for compounds CVM-05-002, **3**, **13**, and **31** (excluding mutant, atypical, and pathogen panel). The inhibitors were tested at 1 μM on a panel of 468 kinases. The results are displayed as red circles with their sizes correlating with the inhibitor's binding affinity (Percent DMSO Control).

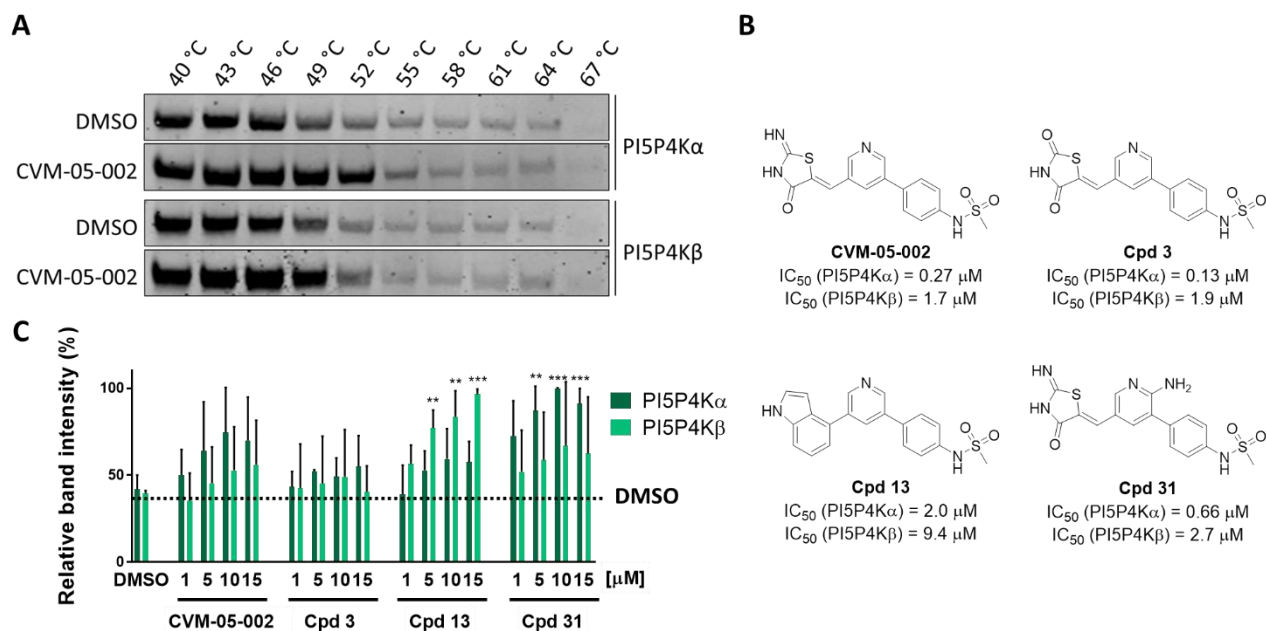


Figure 4. **A.** Western blot of melting curve determination of PI5P4K α and - β . HEK 293T cells were either treated for 1 h with DMSO or 10 μM CVM-05-002. Representative Western blot of two independent repeats. **B.** Structures of selected compounds of the presented SAR study and their biochemical activities. **C.** Quantified relative band intensity (%) of isothermal CETSA experiment (Supporting Figure 10). Shown is the mean of four independent experiments. ** $p < 0.01$, *** $p < 0.001$ by t -test.

1 potentially due to the weaker activity of CMV-05-002 towards
2 this isoform. Consequently, we do not believe that the assay is
3 a good predictor for identifying PI5P4K β activity in the mi-
4 cromolar range at this concentration, but it is still very useful to
5 identify potential off-targets. This is true for all the analogs
6 tested in this assay format.

7 Surprisingly, even though compound **3** is similarly potent to
8 CVM-05-002 in biochemical assays, the change from the 2-imino-
9 thiazolidin-4-one to the thiazolidine-2,4-dione led to a slight
10 selectivity-shift of the inhibitor. With a similar number of off-
11 targets ($S_{35} = 0.03$), compound **3** was not more promiscuous
12 than CVM-05-002, however, its activity shifted from ACVR2A
13 towards MEK3. More importantly, among the lipid kinases, a
14 major off-target, phosphatidylinositol 4-phosphate 5-kinase γ
15 (PI4P5K γ), showed strong binding affinity to compound **3**,
16 while losing affinity for PI5P4K γ . We further confirmed poten-
17 tial off-targets by commercially available biochemical activity
18 assays (Supporting Table 2). This data validated that CVM-05-
19 002 and compound **3** have potent off-target activity for
20 ACVR2B and TGFBR2. Compound **3** showed slightly stronger
21 PI4P5K γ activity as compared to CVM-05-002 by almost 2-
22 fold, which is not as pronounced as in the Ambit KINOMEScan
23 profiling, nonetheless confirming this lipid kinase off-target. As
24 mentioned before, there are no kinase activity assays for
25 PI5P4K γ , however, we have compared binding affinity using
26 K_D values (Supporting Table 2). This data supports our find-
27 ings, that CVM-05-002 is a strong binder of PI5P4K γ with a K_D
28 of 1.6 nM. Interestingly, compound **3** showed a slightly
29 stronger K_D . It should be noted, that we have added our previ-
30 ously reported pan-PI5P4K inhibitor, THZ-P1-2, as a positive
31 control for PI5P4K γ binding (K_D of 4.8 nM), where we have
32 additionally shown covalent engagement of the lipid kinase.¹⁷

33 Comparing the selectivity profile of CVM-05-002 and com-
34 pound **13**, replacing the (*Z*)-methylenethiazolidinone moiety
35 with the bicyclic indole, the change in the left-hand side of the
36 scaffold was able to dial out all seen off-targets of CVM-05-002
37 and resulted in a highly selective compound with strong affinity
38 to PI5P4K γ ($S_{35} = 0.02$), confirmed with a K_D of 3.4 nM. The
39 biochemical activity assays further showed lost off-target activ-
40 ity for ACVR2A/B and TGFBR2 of almost 2-log-fold changes
41 or more. Likewise, the lipid kinase off-target PI4P5K γ activity
42 dropped by 4-fold. In contrast to that, even though we were
43 able to gain selectivity against protein kinases with the addi-
44 tional hinge-binding amino group in compound **31**, this inhibi-
45 tor became a pan-lipid kinase binder ($S_{35} = 0.03$), with strong
46 affinity for PI4P5K γ , 200-times more active on this lipid kinase
47 than compound **13**. Interestingly, this compound exhibited the
48 strongest K_D for PI5P4K γ with 23 pM.

49 **Cellular Target Engagement.** To determine the cellular tar-
50 get engagement of our inhibitors, we established a cellular ther-
51 mal shift assay (CETSA) protocol, which was previously de-
52 scribed.¹⁷ HEK 293T cells were treated with either DMSO or
53 10 μ M of CVM-05-002 for 1 h. The collected cells were then
54 aliquoted and treated at temperatures ranging from 40 to 67 $^{\circ}$ C.
55 Finally, the treated samples were lysed and the soluble protein
56 fraction analyzed *via* Western blot. A representative Western
57 blot is shown in Figure 4A, indicating that 49 $^{\circ}$ C is a suitable
58 temperature for further isothermal CETSA experiments, since
59 the inhibitor treated cells show a strong signal for both,
60 PI5P4K α and β , while the DMSO treated cells show a visible
loss in soluble PI5P4K kinases in comparison. This temperature

was, hence, selected for the following isothermal CETSA ex-
periments.

Summarized in Figure 4C are four independently performed
isothermal CETSA experiments with the previously selected
four PI5P4K inhibitors (Figure 4B, Supporting Figure 4). Com-
pared to DMSO, all compounds, apart from compound **3**, show
at least a slight stabilization of both PI5P4K isoforms in HEK
293T cells with increasing compound concentration. Although
CVM-05-002 shows visible stabilization of PI5P4Ks, the re-
sults are not statistically significant, which is in accordance to
compound's low permeability in a PAMPA assay setup (Sup-
porting Table 4). This was to be expected due to the com-
pound's low LogD value of 0.66. It should, however, be noted,
that the CETSA assay results were rather noisy, leading to rel-
atively high error bars as seen in Figure 4C, which in turn makes
it difficult to get statistical significant results, even though the
increase in soluble protein is visible in the Western blot, indi-
cating some target engagement in HEK293T cells. This lies in
the nature of the assay itself, since the outcome can be influ-
enced by variations in cell density of each repeat or within well-
plates, duration of heating and cooling periods and other fac-
tors.³⁶ Nonetheless, the CETSA assay remains a powerful tool
to confirm overall target engagement in cells.

As expected, compound **13** showed excellent permeability in
the PAMPA assay (Supporting Table 4), which we were able to
confirm in HEK293T cells. In contrast to CVM-05-002 and
compound **3**, compound **13** was able to cause statistically sig-
nificant stabilization of soluble PI5P4K β ($p < 0.01$ by *t*-test).
The visible but only slight effect of compound **13** on PI5P4K α
underlines that the biochemical PI5P4K α and β assays are not
necessarily translating in cells, since the IC_{50} values for
PI5P4K α were generally lower than the ones for the β -isoform.
That said, compound **13** seemed to have a better stabilizing ef-
fect on PI5P4K β in HEK293T cells.

Somewhat surprisingly, compound **31**, only differing from
CVM-05-002 in an additional hinge-binding amino group,
showed strong cellular stabilizing effects of PI5P4K α ($p <$
0.001 by *t*-test). This was unexpected, since the compound is
even more polar than the initial hit compound and is conse-
quently showing similarly bad permeability properties as CVM-
05-002 (Supporting Table 4). Since all compounds tested
showed good microsome stability (Supporting Table 4) and
PAMPA assays do not include active cellular uptake or excre-
tion, nor do we know the effects of the off-target binding of the
inhibitors on PI5P4K activity in cells, it is hard to explain this
strong cellular effect of the compound. It should also be noted
that PI5P4Ks are able to heterodimerize,³⁷ meaning stabiliza-
tion of PI5P4K γ may stabilize PI5P4K α through protein-protein
interactions mediated mechanism, further complicating the de-
tailed interpretation of the CETSA results. We therefore fo-
cused on general activity of the compounds in cells as a measure
of ability to function as a probe in the cellular context in order
to investigate PI5P4Ks.

CONCLUSION

In this study, we have discovered a novel pan-PI5P4K inhib-
itor, CVM-05-002, with low- to sub-micromolar potency based
on a thiazolidinone scaffold, using high-throughput screening
methods of our in-house kinase inhibitor library. Even though
the rhodanine-like scaffold can exhibit PAINS behavior, we
were able to show that the identified hit compound is non-react-
ive, and a highly potent and selective ATP-site directed

inhibitor of the PI5P4K kinases in biochemical and cellular assays. A co-crystal structure of the initial hit with PI5P4K α was used for structure-guided elucidation of the structure-activity relationships to design further analogs based on this newly discovered PI5P4K-binding scaffold and explore its SAR. As a result, we were able to design compound **13**, which lacks the thiazolidinone chemotype, and is a low micromolar PI5P4K inhibitor with excellent selectivity and cellular potency, posing a useful probe to study PI5P4Ks. In summary, we present not only a valuable new scaffold of PI5P4K inhibitors but also provide another example of the significance of rhodanine-based scaffolds for medicinal chemistry campaigns, when coupled with careful validation experiments.

EXPERIMENTAL SECTION

Chemistry Experimental

General Methods. Solvents and all chemicals were purchased from commercial sources and used without further purification. Purifications of intermediates and final compounds were performed, using a preparative HPLC with a Waters Sunfire C18 column (19 mm x 50 mm, 5 μ M) and a gradient of 15–95% MeOH in water (0.05% TFA) over 22 min (28 min total run time) at a flow rate of 20 mL/min. Mass spectra data were obtained on a Waters Acquity UPLC, which was also used to determine the purity of final compounds and is noted for each final compound individually. Proton (^1H) and carbon (^{13}C) NMR spectra were recorded on a 500 MHz Bruker Avance III spectrometer (500 MHz for ^1H ; 126 MHz for ^{13}C). Reported are chemical shifts in ppm (δ) downfield from TMS. Coupling constants (J) are reported in Hz and spin multiplicities are noted as s (singlet), d (doublet), t (triplet), q (quartet), dd (doublet of doublet) or m (multiplet).

General Procedure A: Suzuki Coupling. Boronic acids or respective boronic acid esters (1.1 eq), bromobenzenes (1.0 eq), and Cs_2CO_3 (5.0 eq) were dissolved in a mixture of 1,4-dioxane and water (9:1). The mixture was purged with N_2 for about 10 min. $\text{Pd}(\text{PPh}_3)_2\text{Cl}_2$ (0.1 eq) was added and the reaction was stirred at 100 $^\circ\text{C}$ for 1.5 h. The resulting suspension was filtered through a pad of Celite $^\circledR$ and the solvent was removed *in vacuo*. The crude was further purified by preparative HPLC to yield the desired product.

General Procedure B: Knoevenagel Condensation. To a solution of thiazolidinone derivative (2.0 eq) and aldehyde (1.0 eq) in AcOH was added β -alanine (3.0 eq). The resulting mixture was stirred at 100 $^\circ\text{C}$ for 30 min. After conversion the precipitated product was filtered and purified by preparative HPLC to yield the desired product.

***N*-(4-(5-formylpyridin-3-yl)phenyl)methanesulfonamide (2a).** The intermediate was synthesized after General procedure A, starting from 5-bromonicotinaldehyde (**1a**) and *N*-(4-(4,4,5,5-tetramethyl-1,3,2-dioxaborolan-2-yl)phenyl)methanesulfonamide to yield a yellow-brown oil (84%). MS (ESI) m/z calc. for $\text{C}_{13}\text{H}_{12}\text{N}_2\text{O}_3\text{S}$ [$\text{M}+\text{H}$] $^+$ 277.06; found 277.26.

***N*-(4-(5-bromopyridin-3-yl)phenyl)methanesulfonamide (2b).** The intermediate was synthesized after General procedure A, starting from 3,5-dibromopyridine (**1b**) and *N*-(4-(4,4,5,5-tetramethyl-1,3,2-dioxaborolan-2-yl)phenyl)methanesulfonamide to yield a light-ochre solid (55%). MS (ESI) m/z calc. for $\text{C}_{12}\text{H}_{11}\text{BrN}_2\text{O}_2\text{S}$ [$\text{M}+\text{H}$] $^+$ 326.98; found 327.11.

***N*-(4-(5-aminopyridin-3-yl)phenyl)methanesulfonamide (2c).** The intermediate was synthesized after General procedure

A, starting from 5-bromopyridin-3-amine (**1c**) and *N*-(4-(4,4,5,5-tetramethyl-1,3,2-dioxaborolan-2-yl)phenyl)methanesulfonamide to yield a white solid (206 mg, 100% = 187 mg). MS (ESI) m/z calc. for $\text{C}_{12}\text{H}_{13}\text{N}_3\text{O}_2\text{S}$ [$\text{M}+\text{H}$] $^+$ 264.08; found 264.27.

(Z)-*N*-(4-(5-((2-imino-4-oxothiazolidin-5-ylidene)methyl)pyridin-3-yl)phenyl)methanesulfonamide (CVM-05-002). The title compound was synthesized after General procedure B, starting from intermediate **2a** and 2-iminothiazolidin-4-one to yield a light-yellow solid (33%). MS (ESI) m/z calc. for $\text{C}_{16}\text{H}_{14}\text{N}_4\text{O}_3\text{S}_2$ [$\text{M}+\text{H}$] $^+$ 375.06; found 375.20. ^1H NMR (500 MHz, DMSO- d_6) δ 9.98 (s, 1H), 9.57 (s, 1H), 9.24 (s, 1H), 8.88 (s, 1H), 8.77 (s, 1H), 8.15 (s, 1H), 7.76 (d, J = 8.5 Hz, 2H), 7.70 (s, 1H), 7.35 (d, J = 8.5 Hz, 2H), 3.06 (s, 3H). ^{13}C NMR (126 MHz, DMSO) δ 175.67, 149.25, 147.98, 139.45, 135.59, 133.82, 132.58, 132.02, 130.84, 128.45, 125.93, 120.41, 40.92; purity 100%.

(Z)-*N*-(4-(5-((2,4-dioxothiazolidin-5-ylidene)methyl)pyridin-3-yl)phenyl)methanesulfonamide (3). The title compound was synthesized after General procedure B, starting from intermediate **2a** and thiazolidine-2,4-dione to yield a light-yellow solid (12%). MS (ESI) m/z calc. for $\text{C}_{16}\text{H}_{13}\text{N}_3\text{O}_4\text{S}_2$ [$\text{M}+\text{H}$] $^+$ 376.04; found 376.18. ^1H NMR (500 MHz, DMSO- d_6) δ 12.75 (s, 1H), 9.99 (s, 1H), 8.93 (d, J = 1.8 Hz, 1H), 8.77 (s, 1H), 8.16 (s, 1H), 7.90 (s, 1H), 7.77 (d, J = 8.5 Hz, 2H), 7.36 (d, J = 8.5 Hz, 2H), 3.06 (s, 3H). ^{13}C NMR (126 MHz, DMSO) δ 167.96, 167.62, 149.44, 148.71, 139.54, 135.65, 134.25, 131.65, 129.93, 128.89, 128.52, 126.87, 120.32; purity 100%.

(Z)-*N*-(4-(5-((2,4-dioxooxazolidin-5-ylidene)methyl)pyridin-3-yl)phenyl)methanesulfonamide (4). Intermediate **2a** (0.145 mmol, 1.0 eq), oxazolidine-2,4-dione (0.174 mmol, 1.2 eq), and piperidine (0.044 mmol, 0.3 eq) were dissolved in EtOH (1 mL) and stirred at 100 $^\circ\text{C}$ overnight. The crude was purified by preparative HPLC to yield the title compound as a brown solid (4%). MS (ESI) m/z calc. for $\text{C}_{16}\text{H}_{13}\text{N}_3\text{O}_5\text{S}$ [$\text{M}+\text{H}$] $^+$ 360.06; found 360.48. ^1H NMR (500 MHz, DMSO- d_6) δ 9.96 (s, 2H), 8.94 (s, 1H), 8.53 (s, 1H), 8.03 (s, 1H), 7.77 (d, J = 8.6 Hz, 2H), 7.33 (d, J = 8.6 Hz, 2H), 3.05 (s, 3H); purity 90%.

(E)-*N*-(4-(5-((2,5-dioxopyrrolidin-3-ylidene)methyl)pyridin-3-yl)phenyl)methanesulfonamide (5). Intermediate **2a** (0.145 mmol, 1.0 eq), maleimide (0.145 mmol, 1.0 eq), and triphenylphosphine (0.145 mmol, 1.0 eq) were dissolved in DCM (1 mL) and stirred at room temperature overnight. The crude was purified by preparative HPLC to yield the title compound as an ivory solid (4%). MS (ESI) m/z calc. for $\text{C}_{17}\text{H}_{15}\text{N}_3\text{O}_4\text{S}$ [$\text{M}+\text{H}$] $^+$ 358.09; found 358.44. ^1H NMR (500 MHz, DMSO- d_6) δ 11.54 (s, 1H), 9.96 (s, 1H), 8.89 (s, 1H), 8.79 (s, 1H), 8.21 (s, 1H), 7.81 (d, J = 8.5 Hz, 2H), 7.49 (s, 1H), 7.35 (d, J = 8.5 Hz, 2H), 3.84 (d, J = 2.4 Hz, 2H), 3.05 (s, 3H); purity 98%.

***N*-(4-(5-(2-oxoindolin-4-yl)pyridin-3-yl)phenyl)methanesulfonamide (6).** The title compound was synthesized after General procedure A, starting from intermediate **2b** and (2-oxoindolin-4-yl)boronic acid pinacol ester to yield an orange-brown solid (1%). MS (ESI) m/z calc. for $\text{C}_{20}\text{H}_{17}\text{N}_3\text{O}_3\text{S}$ [$\text{M}+\text{H}$] $^+$ 380.11; found 380.22. ^1H NMR (500 MHz, DMSO- d_6) δ 10.53 (s, 1H), 9.94 (s, 1H), 8.89 (s, 1H), 8.76 (s, 1H), 8.20 (s, 1H), 7.82 (d, J = 8.6 Hz, 2H), 7.40 – 7.30 (m, 3H), 7.17 (d, J = 7.7 Hz, 1H), 6.90 (d, J = 7.5 Hz, 1H), 3.73 (s, 2H), 3.05 (s, 3H); purity 94%.

***N*-(3-(5-(4-(methylsulfonamido)phenyl)pyridin-3-yl)phenyl)acetamide (7).** The title compound was synthesized after General procedure A, starting from intermediate **2b** and (3-

acetamidophenyl)boronic acid to yield a white solid (37%). MS (ESI) m/z calc. for $C_{20}H_{19}N_3O_3S$ $[M+H]^+$ 382.12; found 382.28. 1H NMR (500 MHz, DMSO- d_6) δ 10.15 (s, 1H), 10.04 (s, 1H), 9.03 (s, 1H), 8.93 (s, 1H), 8.49 (s, 1H), 8.03 (s, 1H), 7.88 (d, J = 8.7 Hz, 2H), 7.67 (d, J = 8.1 Hz, 1H), 7.54 (d, J = 7.8 Hz, 1H), 7.47 (t, J = 7.9 Hz, 1H), 7.37 (d, J = 8.7 Hz, 2H), 3.07 (s, 3H), 2.08 (s, 3H); purity 100%.

***N*-(4-(5-(4-(3-methylureido)phenyl)pyridin-3-yl)phenyl)methanesulfonamide (8)**. The title compound was synthesized after General procedure A, starting from intermediate **2b** and (4-(3-methylureido)phenyl)boronic acid to yield a light-yellow solid (37%). MS (ESI) m/z calc. for $C_{20}H_{20}N_4O_3S$ $[M+H]^+$ 397.13; found 397.21. 1H NMR (500 MHz, DMSO- d_6) δ 9.97 (s, 1H), 8.88 (s, 1H), 8.86 (s, 1H), 8.73 (s, 1H), 8.38 (s, 1H), 7.86 (d, J = 8.5 Hz, 2H), 7.76 (d, J = 8.9 Hz, 2H), 7.56 (d, J = 8.9 Hz, 2H), 7.35 (d, J = 8.5 Hz, 2H), 6.10 (d, J = 4.0 Hz, 1H), 3.06 (s, 3H), 2.66 (d, J = 3.2 Hz, 3H); purity 100%.

***N*-(3-((5-(4-(methylsulfonamido)phenyl)pyridin-3-yl)oxy)phenyl)acetamide (9)**. Intermediate **2b** (0.122 mmol, 1.0 eq), *N*-(3-hydroxyphenyl)acetamide (0.24 mmol, 2.0 eq), K_2CO_3 (0.24 mmol, 2.0 eq), and CuI (0.0122 mmol, 0.1 eq) were dissolved in DMF (0.5 mL) and stirred at 120 °C for 2 days. The crude was purified by preparative HPLC to yield the title compound as a brown solid (3%). MS (ESI) m/z calc. for $C_{20}H_{19}N_3O_4S$ $[M+H]^+$ 398.12; found 398.29. 1H NMR (500 MHz, DMSO- d_6) δ 10.04 (s, 1H), 9.95 (s, 1H), 7.98 – 7.68 (m, 4H), 7.42 (s, 1H), 7.38 – 7.29 (m, 5H), 6.78 (s, 1H), 3.03 (s, 3H), 2.01 (s, 3H); purity 92%.

***N*-(3-((5-(4-(methylsulfonamido)phenyl)pyridin-3-yl)amino)phenyl)acetamide (10)**. Intermediate **2c** (0.152 mmol, 1.0 eq), *N*-(3-bromophenyl)acetamide (0.182 mmol, 1.2 eq), K_2CO_3 (0.38 mmol, 2.5 eq), and X-Phos (0.023 mmol, 0.15 eq) were dissolved in 1,4-dioxane (1.0 mL). The mixture was purged with N_2 for about 10 minutes, $Pd_2(dba)_3$ (0.0076 mmol, 0.05 eq) was added, and the reaction was stirred at 80 °C overnight. The crude was purified by preparative HPLC to yield the title compound as a yellow solid (7%). MS (ESI) m/z calc. for $C_{20}H_{20}N_4O_3S$ $[M+H]^+$ 397.13; found 397.54. 1H NMR (500 MHz, DMSO- d_6) δ 9.96 (s, 1H), 9.92 (s, 1H), 8.71 (s, 1H), 7.78 (s, 1H), 7.71 (d, J = 8.5 Hz, 2H), 7.66 (s, 1H), 7.32 (d, J = 8.5 Hz, 2H), 7.24 – 7.18 (m, 1H), 7.11 (s, 1H), 7.05 (d, J = 8.2 Hz, 1H), 7.01 (s, 1H), 6.83 (d, J = 8.0 Hz, 1H), 3.05 (s, 3H), 2.04 (s, 3H); purity 100%.

4-(5-bromopyridin-3-yl)-1*H*-indole (12a). The intermediate was synthesized after General procedure A, starting from 4-bromo-1*H*-indole and (5-bromopyridin-3-yl)boronic acid (**11**) to yield a yellow-brown oil (18%). MS (ESI) m/z calc. for $C_{13}H_9BrN_2$ $[M+H]^+$ 273.00; found 273.32.

5-(5-bromopyridin-3-yl)-1*H*-indole (12b). The intermediate was synthesized after General procedure A, starting from 5-bromo-1*H*-indole and (5-bromopyridin-3-yl)boronic acid (**11**) to yield a yellow-brown oil (9%). MS (ESI) m/z calc. for $C_{13}H_9BrN_2$ $[M+H]^+$ 273.00; found 273.33.

6-(5-bromopyridin-3-yl)-1*H*-indole (12c). The intermediate was synthesized after General procedure A, starting from 6-bromo-1*H*-indole and (5-bromopyridin-3-yl)boronic acid (**11**) to yield a yellow-orange solid (14%). MS (ESI) m/z calc. for $C_{13}H_9BrN_2$ $[M+H]^+$ 273.00; found 273.34.

***N*-(4-(5-(1*H*-indol-4-yl)pyridin-3-yl)phenyl)methanesulfonamide (13)**. The title compound was synthesized after General procedure A, starting from intermediate **12a** and *N*-(4-

(4,4,5,5-tetramethyl-1,3,2-dioxaborolan-2-yl)phenyl)methanesulfonamide to yield an ochre solid (19%). MS (ESI) m/z calc. for $C_{20}H_{17}N_3O_2S$ $[M+H]^+$ 364.11; found 364.14. 1H NMR (500 MHz, DMSO- d_6) δ 11.39 (s, 1H), 9.97 (s, 1H), 8.94 (s, 1H), 8.90 (s, 1H), 8.35 (s, 1H), 7.85 (d, J = 8.9 Hz, 2H), 7.61 (d, J = 8.5 Hz, 1H), 7.51 (d, J = 7.3 Hz, 1H), 7.49 – 7.46 (m, 1H), 7.36 (d, J = 8.9 Hz, 2H), 7.30 – 7.23 (m, 1H), 6.61 (s, 1H), 3.06 (s, 3H); purity 94%.

***N*-(5-(5-(1*H*-indol-4-yl)pyridin-3-yl)phenyl)methanesulfonamide (14)**. The title compound was synthesized after General procedure A, starting from intermediate **12b** and *N*-(4-(4,4,5,5-tetramethyl-1,3,2-dioxaborolan-2-yl)phenyl)methanesulfonamide to yield an orange solid (27%). MS (ESI) m/z calc. for $C_{20}H_{17}N_3O_2S$ $[M+H]^+$ 364.11; found 364.14. 1H NMR (500 MHz, DMSO- d_6) δ 11.30 (s, 1H), 9.98 (s, 1H), 8.94 (s, 1H), 8.89 (s, 1H), 8.42 (s, 1H), 7.88 (d, J = 8.9 Hz, 2H), 7.84 (s, 1H), 7.70 (d, J = 8.2 Hz, 1H), 7.48 (d, J = 10.1 Hz, 1H), 7.46 – 7.41 (m, 1H), 7.37 (d, J = 8.5 Hz, 2H), 6.50 (s, 1H), 3.06 (s, 3H); purity 92%.

***N*-(6-(5-(1*H*-indol-4-yl)pyridin-3-yl)phenyl)methanesulfonamide (15)**. The title compound was synthesized after General procedure A, starting from intermediate **12c** and *N*-(4-(4,4,5,5-tetramethyl-1,3,2-dioxaborolan-2-yl)phenyl)methanesulfonamide to yield an off-white solid (21%). MS (ESI) m/z calc. for $C_{20}H_{17}N_3O_2S$ $[M+H]^+$ 364.11; found 364.13. 1H NMR (500 MHz, DMSO- d_6) δ 11.28 (s, 1H), 9.99 (s, 1H), 8.97 (s, 1H), 8.89 (s, 1H), 8.50 (s, 1H), 8.07 (s, 1H), 7.90 (d, J = 8.5 Hz, 2H), 7.59 (d, J = 8.9 Hz, 1H), 7.55 (d, J = 8.2 Hz, 1H), 7.46 – 7.42 (m, 1H), 7.37 (d, J = 8.5 Hz, 2H), 6.54 (s, 1H), 3.07 (s, 3H); purity 95%.

4-(5-formylpyridin-3-yl)-*N*-methylbenzenesulfonamide (17a). The intermediate was synthesized after General procedure A, starting from 5-bromonicotinaldehyde (**16**) and (4-(*N*-methylsulfamoyl)phenyl)boronic acid to yield a colorless oil (76%). MS (ESI) m/z calc. for $C_{13}H_{12}N_2O_3S$ $[M+H]^+$ 277.06; found 277.40.

5-(4-(methylsulfonyl)phenyl)nicotinaldehyde (17b). The intermediate was synthesized after General procedure A, starting from 5-bromonicotinaldehyde (**16**) and (4-(methylsulfonyl)phenyl)boronic acid to yield a colorless oil (74%). MS (ESI) m/z calc. for $C_{13}H_{11}NO_3S$ $[M+H]^+$ 262.05; found 262.38.

***N*-(4-(5-formylpyridin-3-yl)phenyl)acetamide (17c)**. The intermediate was synthesized after General procedure A, starting from 5-bromonicotinaldehyde (**16**) and (4-acetamidophenyl)boronic acid to yield a yellow oil (88%). MS (ESI) m/z calc. for $C_{14}H_{12}N_2O_2$ $[M+H]^+$ 241.10; found 241.27.

1-(4-(5-formylpyridin-3-yl)phenyl)-3-methylurea (17d). The intermediate was synthesized after General procedure A, starting from 5-bromonicotinaldehyde (**16**) and (4-(3-methylureido)phenyl)boronic acid pinacol ester to yield a yellow oil (63%). MS (ESI) m/z calc. for $C_{14}H_{13}N_3O_2$ $[M+H]^+$ 256.11; found 256.46.

***N*-(3-(5-formylpyridin-3-yl)phenyl)acetamide (17e)**. The intermediate was synthesized after General procedure A, starting from 5-bromonicotinaldehyde (**16**) and (3-acetamidophenyl)boronic acid to yield a light-yellow oil (71%). MS (ESI) m/z calc. for $C_{14}H_{12}N_2O_2$ $[M+H]^+$ 241.10; found 241.27.

5-(4-(trifluoromethoxy)phenyl)nicotinaldehyde (17f). The intermediate was synthesized after General procedure A, starting from 5-bromonicotinaldehyde (**16**) and (4-

(trifluoromethoxy)phenyl)boronic acid to yield a yellow oil (93%). MS (ESI) m/z calc. for $C_{13}H_8F_3NO_2$ $[M+H]^+$ 268.06; found 268.38.

5-(4-(trifluoromethyl)phenyl)nicotinaldehyde (17g). The intermediate was synthesized after General procedure A, starting from 5-bromonicotinaldehyde (**16**) and 4-(trifluoromethyl)phenyl)boronic acid to yield a light-yellow oil (64%). MS (ESI) m/z calc. for $C_{13}H_8F_3NO$ $[M+H]^+$ 252.06; found 252.25.

5-(4-fluorophenyl)nicotinaldehyde (17h). The intermediate was synthesized after General procedure A, starting from 5-bromonicotinaldehyde (**16**) and 4-fluorophenyl)boronic acid to yield a light-yellow oil (86 mg, 100% = 85 mg). MS (ESI) m/z calc. for $C_{12}H_8FNO$ $[M+H]^+$ 202.07; found 202.18.

5-(4-(dimethylamino)phenyl)nicotinaldehyde (17i). The intermediate was synthesized after General procedure A, starting from 5-bromonicotinaldehyde (**16**) and 4-(dimethylamino)phenyl)boronic acid to yield a red-orange oil (114 mg, 100% = 92 mg). MS (ESI) m/z calc. for $C_{14}H_{14}N_2O$ $[M+H]^+$ 227.12; found 227.42.

5-(4-methoxynaphthalen-1-yl)nicotinaldehyde (17j). The intermediate was synthesized after General procedure A, starting from 5-bromonicotinaldehyde (**16**) and 4-methoxynaphthalen-1-yl)boronic acid to yield a yellow-orange oil (71%). MS (ESI) m/z calc. for $C_{17}H_{13}NO_2$ $[M+H]^+$ 264.10; found 264.43.

(Z)-4-(5-((2-imino-4-oxothiazolidin-5-ylidene)methyl)pyridin-3-yl)-N-methylbenzenesulfonamide (18). The title compound was synthesized after General procedure B, starting from intermediate **17a** and 2-iminothiazolidin-4-one to yield a white solid (19%). MS (ESI) m/z calc. for $C_{16}H_{14}N_4O_2S_3$ $[M+H]^+$ 375.06; found 375.42. 1H NMR (500 MHz, DMSO- d_6) δ 9.59 (s, 1H), 9.26 (s, 1H), 8.97 (s, 1H), 8.86 (s, 1H), 8.27 (t, $J = 2.0$ Hz, 1H), 8.02 (d, $J = 8.5$ Hz, 2H), 7.91 (d, $J = 8.5$ Hz, 2H), 7.73 (s, 1H), 7.56 (q, $J = 4.9$ Hz, 1H), 2.46 (d, $J = 5.2$ Hz, 3H); purity 98%.

(Z)-2-imino-5-((5-(4-(methylsulfonyl)phenyl)pyridin-3-yl)methylene)thiazolidin-4-one (19). The title compound was synthesized after General procedure B, starting from intermediate **17b** and 2-iminothiazolidin-4-one to yield a white solid (9%). MS (ESI) m/z calc. for $C_{16}H_{13}N_3O_3S_2$ $[M+H]^+$ 360.05; found 360.38. 1H NMR (500 MHz, DMSO- d_6) δ 9.59 (s, 1H), 9.27 (s, 1H), 8.99 (s, 1H), 8.88 (s, 1H), 8.28 (s, 1H), 8.11 – 8.01 (m, 4H), 7.74 (s, 1H), 3.29 (s, 3H); purity 97%.

(Z)-N-(4-(5-((2-imino-4-oxothiazolidin-5-ylidene)methyl)pyridin-3-yl)phenyl)acetamide (20). The title compound was synthesized after General procedure B, starting from intermediate **17c** and 2-iminothiazolidin-4-one to yield an off-white solid (4%). MS (ESI) m/z calc. for $C_{17}H_{14}N_4O_2S$ $[M+H]^+$ 339.09; found 339.18. 1H NMR (500 MHz, DMSO- d_6) δ 10.11 (s, 1H), 9.57 (s, 1H), 9.23 (s, 1H), 8.88 (d, $J = 2.2$ Hz, 1H), 8.75 (d, $J = 2.1$ Hz, 1H), 8.15 (t, $J = 2.2$ Hz, 1H), 7.76 – 7.71 (m, 4H), 7.70 (s, 1H), 2.08 (s, 3H); purity 100%.

(Z)-1-(4-(5-((2-imino-4-oxothiazolidin-5-ylidene)methyl)pyridin-3-yl)phenyl)-3-methylurea (21). The title compound was synthesized after General procedure B, starting from intermediate **17d** and 2-iminothiazolidin-4-one to yield an ivory solid (18%). MS (ESI) m/z calc. for $C_{17}H_{15}N_5O_2S$ $[M+H]^+$ 354.10; found 354.42. 1H NMR (500 MHz, DMSO- d_6) δ 9.56 (s, 1H), 9.23 (s, 1H), 8.87 (s, 1H), 8.75 – 8.67 (m, 2H), 8.12 (d, $J = 2.1$ Hz, 1H), 7.70 (s, 1H), 7.65 (d, $J = 8.8$ Hz, 2H), 7.56 (d, $J = 8.8$ Hz, 2H), 6.09 (t, $J = 4.7$ Hz, 1H), 2.66 (d, $J = 4.5$ Hz, 3H); purity 100%.

(Z)-N-(3-(5-((2-imino-4-oxothiazolidin-5-ylidene)methyl)pyridin-3-yl)phenyl)acetamide (22). The title compound was synthesized after General procedure B, starting from intermediate **17e** and 2-iminothiazolidin-4-one to yield an off-white solid (4%). MS (ESI) m/z calc. for $C_{17}H_{14}N_4O_2S$ $[M+H]^+$ 339.09; found 339.16. 1H NMR (500 MHz, DMSO- d_6) δ 10.12 (s, 1H), 9.58 (s, 1H), 9.26 (s, 1H), 8.82 (s, 2H), 8.09 (s, 1H), 7.95 (s, 1H), 7.72 (s, 1H), 7.66 (d, $J = 8.5$ Hz, 1H), 7.46 (t, $J = 7.9$ Hz, 1H), 7.41 (d, $J = 7.6$ Hz, 1H), 2.08 (s, 3H); purity 100%.

(Z)-2-imino-5-((5-(4-(trifluoromethoxy)phenyl)pyridin-3-yl)methylene)thiazolidin-4-one (23). The title compound was synthesized after General procedure B, starting from intermediate **17f** and 2-iminothiazolidin-4-one to yield a light-orange solid (11%). MS (ESI) m/z calc. for $C_{16}H_{10}F_3N_3O_2S$ $[M+H]^+$ 366.05; found 366.40. 1H NMR (500 MHz, DMSO- d_6) δ 9.58 (s, 1H), 9.25 (s, 1H), 8.93 (s, 1H), 8.83 (s, 1H), 8.20 (t, $J = 2.0$ Hz, 1H), 7.95 – 7.88 (m, 2H), 7.72 (s, 1H), 7.54 (d, $J = 7.9$ Hz, 2H); purity 96%.

(Z)-2-imino-5-((5-(4-(trifluoromethyl)phenyl)pyridin-3-yl)methylene)thiazolidin-4-one (24). The title compound was synthesized after General procedure B, starting from intermediate **17g** and 2-iminothiazolidin-4-one to yield a white solid (12%). MS (ESI) m/z calc. for $C_{16}H_{10}F_3N_3OS$ $[M+H]^+$ 350.06; found 350.15. 1H NMR (500 MHz, DMSO- d_6) δ 9.59 (s, 1H), 9.27 (s, 1H), 8.97 (s, 1H), 8.86 (s, 1H), 8.26 (t, $J = 2.0$ Hz, 1H), 8.02 (d, $J = 8.2$ Hz, 2H), 7.90 (d, $J = 8.2$ Hz, 2H), 7.73 (s, 1H); purity 100%.

(Z)-5-((5-(4-fluorophenyl)pyridin-3-yl)methylene)-2-iminothiazolidin-4-one (25). The title compound was synthesized after General procedure B, starting from intermediate **17h** and 2-iminothiazolidin-4-one to yield a white solid (4%). MS (ESI) m/z calc. for $C_{15}H_{10}FN_3OS$ $[M+H]^+$ 300.06; found 300.15. 1H NMR (500 MHz, DMSO- d_6) δ 9.58 (s, 1H), 9.25 (s, 1H), 8.89 (d, $J = 2.1$ Hz, 1H), 8.80 (s, 1H), 8.16 (t, $J = 2.0$ Hz, 1H), 7.88 – 7.77 (m, 2H), 7.71 (s, 1H), 7.39 (t, $J = 8.9$ Hz, 2H); purity 97%.

(Z)-5-((5-(4-(dimethylamino)phenyl)pyridin-3-yl)methylene)-2-iminothiazolidin-4-one (26). The title compound was synthesized after General procedure B, starting from intermediate **17i** and 2-iminothiazolidin-4-one to yield an orange-red solid (13%). MS (ESI) m/z calc. for $C_{17}H_{16}N_4OS$ $[M+H]^+$ 325.11; found 325.43. 1H NMR (500 MHz, DMSO- d_6) δ 9.57 (s, 1H), 9.25 (s, 1H), 8.87 (s, 1H), 8.69 (s, 1H), 8.14 (t, $J = 2.1$ Hz, 1H), 7.70 (s, 1H), 7.64 (d, $J = 8.8$ Hz, 2H), 6.86 (d, $J = 8.8$ Hz, 2H), 2.98 (s, 6H); purity 96%.

(Z)-2-imino-5-((5-(4-methoxynaphthalen-1-yl)pyridin-3-yl)methylene)thiazolidin-4-one (27). The title compound was synthesized after General procedure B, starting from intermediate **17j** and 2-iminothiazolidin-4-one to yield an orange solid (21%). MS (ESI) m/z calc. for $C_{20}H_{15}N_3O_2S$ $[M+H]^+$ 362.10; found 362.44. 1H NMR (500 MHz, DMSO- d_6) δ 9.54 (s, 1H), 9.18 (s, 1H), 8.89 (s, 1H), 8.68 (s, 1H), 8.33 – 8.24 (m, 1H), 7.99 (s, 1H), 7.79 – 7.75 (m, 1H), 7.75 (s, 1H), 7.61 – 7.56 (m, 2H), 7.50 (d, $J = 7.9$ Hz, 1H), 7.12 (d, $J = 7.9$ Hz, 1H), 4.05 (s, 3H); purity 100%.

N-(4-(6-amino-5-formylpyridin-3-yl)phenyl)methanesulfonamide (29a). The intermediate was synthesized after General procedure A, starting from 2-amino-5-bromonicotinaldehyde (**28a**) and *N*-(4-(4,4,5,5-tetramethyl-1,3,2-dioxaborolan-2-yl)phenyl)methanesulfonamide (**1**) to yield a yellow oil (74%). MS (ESI) m/z calc. for $C_{13}H_{13}N_3O_3S$ $[M+H]^+$ 292.08; found 292.16.

***N*-(4-(2-amino-5-formylpyridin-3-yl)phenyl)methanesulfonamide (29b)**. The intermediate was synthesized after General procedure A, starting from 6-amino-5-bromonicotinaldehyde (**28b**) and *N*-(4-(4,4,5,5-tetramethyl-1,3,2-dioxaborolan-2-yl)phenyl)methanesulfonamide (**1**) to yield a light-yellow solid (61%). MS (ESI) *m/z* calc. for C₁₃H₁₃N₃O₃S [M+H]⁺ 292.08; found 292.23.

(Z)-*N*-(4-(6-amino-5-((2-imino-4-oxothiazolidin-5-ylidene)methyl)pyridin-3-yl)phenyl)methanesulfonamide (30). The title compound was synthesized after General procedure B, starting from intermediate **29a** and 2-iminothiazolidin-4-one to yield a yellow solid (22%). MS (ESI) *m/z* calc. for C₁₆H₁₅N₅O₃S₂ [M+H]⁺ 390.07; found 390.24. ¹H NMR (500 MHz, DMSO-*d*₆) δ 9.85 (s, 1H), 9.36 (s, 1H), 9.11 (s, 1H), 8.59 (d, *J* = 2.3 Hz, 1H), 8.24 (dd, *J* = 7.5, 2.3 Hz, 1H), 7.67 – 7.53 (m, 4H), 7.34 – 7.27 (m, 3H), 3.03 (s, 3H); purity 86%.

(Z)-*N*-(4-(2-amino-5-((2-imino-4-oxothiazolidin-5-ylidene)methyl)pyridin-3-yl)phenyl)methanesulfonamide (31). The title compound was synthesized after General procedure B, starting from intermediate **29b** and 2-iminothiazolidin-4-one to yield a yellow solid (10%). MS (ESI) *m/z* calc. for C₁₆H₁₅N₅O₃S₂ [M+H]⁺ 390.07; found 390.23. ¹H NMR (500 MHz, DMSO-*d*₆) δ 9.96 (s, 1H), 9.39 (s, 1H), 9.03 (s, 1H), 8.26 (d, *J* = 2.1 Hz, 1H), 7.60 (d, *J* = 2.1 Hz, 1H), 7.53 (s, 1H), 7.49 – 7.42 (m, 2H), 7.35 – 7.32 (m, 2H), 7.07 (s, 2H), 3.06 (s, 3H); purity 100%.

Biochemical Experimental

High-Throughput Screen. Screenings were performed according to previously described protocols.¹² DPPS and PI5P (Echelon Biosciences) (2:1) were dissolved in DMSO (333 mL/mg). 63 μL of DMSO was added to 1,255 μL of buffer 1 (30 mM Hepes pH 7.4, 1 mM EGTA, 0.1% CHAPS) and 2,868 μL of buffer 2 (46 mM Hepes pH 7.4, 0.1% CHAPS). This could be adjusted to sample numbers. PI5P4Kα enzyme was added to the buffer mixture at 32 nM concentration. 10 μL were dispensed into white 384-well plates (Corning #3824) and 100 nL of compound solution (in DMSO) were transferred by a pintool (JANUS, PerkinElmer). The reaction was initiated with the addition of 5 μL of 15 μM ATP (Promega) and PI5P/DPPS (at 0.06 μg/μL and 0.12 μg/μL, respectively) in buffer 3 (20 mM Hepes pH 7.4, 60 mM MgCl₂, and 0.1% CHAPS). The final concentration of DMSO in the reaction was less than 5%. The resulting mixture was incubated at room temperature in the dark for one hour. 5 μL ADP-Glo reagent 1 were added to stop the reaction and remove remaining ATP. After 45 min, 10 μL ADP-Glo reagent 2 were added and incubated for 30 minutes. The luminescence intensity (RLU) was then read on an EnVision 2104 Multilabel Plate Reader (PerkinElmer). IC₅₀ values were determined using GraphPad Prism 7.04 and non-linear regression curve fit.

Protein Expression and Purification. Recombinant PI5P4Kα, β, and γ were obtained as described before.¹⁶

Mass Spectrometry. Recombinant PI5P4Kα/β were incubated with 10 μM CVM-05-002, THZ-P1-2 (positive control), or DMSO and analyzed by LC/MS as previously described,¹⁶ except that all samples were incubated at room temperature for 2 h, and UniDec³⁸ was used to deconvolute the protein mass spectra.

X-ray Crystallography and Structure Determination. PI5P4Kα was co-crystallized with CVM-05-002 using similar conditions as previously described.¹⁶ A two-fold excess of

Table 4. Data collection and Refinement Statistics

PI5P4Kα/CVM-05-002	
Wavelength (Å)	0.9792
Resolution Range (Å)	45.37 – 1.71 (1.771 – 1.71)
Space Group	<i>P</i> 1 21 1
Unit Cell Constants a, b, c, α, β, γ	44.23 Å 88.58 Å 105.78 Å 90° 92.91° 90°
Total Reflections	291561 (29776)
Unique Reflections	85988 (8587)
Multiplicity	3.4 (3.5)
Completeness (%)	97.72 (97.59)
Mean <i>I</i> /σ(<i>I</i>)	12.42 (1.34)
Wilson B-factor	32.73
<i>R</i> _{merge}	0.04003 (1.022)
<i>R</i> _{meas}	0.04773 (1.207)
<i>R</i> _{pim}	0.02566 (0.6364)
CC1/2	0.999 (0.754)
CC*	1 (0.927)
Reflections Used in Refinement	85916 (8579)
Reflections Used for <i>R</i> _{free}	4198 (366)
<i>R</i> _{work}	0.1767 (0.3611)
<i>R</i> _{free}	0.2032 (0.3938)
CC(work)	0.966 (0.878)
CC(free)	0.947 (0.833)
No. of Non-hydrogen Atoms	5611
Macromolecules	5203
Ligands	50
Solvent	358
Protein Residues	628
RMS(bonds)	0.016
RMS(angles)	1.73
Ramachandran favored (%)	97.39
Ramachandran allowed (%)	2.45
Ramachandran outliers (%)	0.16
Rotamer outliers (%)	0.17
Clashscore	10.58
Average B-Factor	51.85
Macromolecules	52.05
Ligands	46.78
Solvent	49.78
No. of TLS Groups	15

inhibitor was mixed with 500 μM protein and crystallized by sitting-drop vapor diffusion as described. The buffer contained 2 M NH₄ (pH 6.5). Crystals were transferred briefly into crystallization buffer, containing 25% glycerol prior to flash-freezing in liquid nitrogen. Diffraction data from complex crystals were collected at beamline 24ID of the NE-CAT at the

Advanced Photon Source (Argonne National Laboratory). Data sets were integrated and scaled using XDS (Kabsch, 2010). Structures were solved by molecular replacement using the program Phaser. The ligand was positioned manually and refined using Buster and Rhotit. Iterative manual model building and refinement using Phenix and Coot led to a model with excellent statistics, including a maximum diffraction of 1.71 Å.

Protein Structure Alignment. The above describe co-crystal structure of PI5P4K α with CVM-05-002 was aligned with the PDB structures of PI5P4K β (PDB ID: 3WZZ) and PI5P4K γ (PDB ID: 2GK9.A) using the alignment function in PyMOL™ 2.0.5 – Incentive Product Copyright Schrodinger, LLC.

Biological Evaluation. Materials and Methods. All compounds were initially sourced from the National Center for Advancing Translational Studies (NCATS)/National Institutes of Health (NIH). Shipped compounds from NCATS were subjected to quality control by LC/UV, LC/MS, or HRMS, unless otherwise noted, and exhibited >90% purity by peak area or m/z^2 .

Data analysis was performed as previously described.¹⁷

ADP-Glo™ Kinase Assay (PI5P4K α). GDP Transcreeper Assay (PI5P4K β). Protocols for screens and counterscreens were previously reported.¹⁷

Kinome Profiling. Protocols for the KINOMEScan are available from DiscoverX. *Treespot* images were generated, using *TREEspot*™ Software Tool, and reprinted with permission from KINOMEScan®, a division of DiscoverX Corporation, ©DISCOVERX CORPORATION 2010. All compounds were tested at a concentration of 1 μ M.

IC₅₀ Evaluation of Off-targets. Biochemical IC₅₀s of identified off-targets were determined using the commercially available LanthaScreen® or Adapta™ offered by Invitrogen (Thermo Fisher Scientific).

K_D Evaluation for PI5P4K γ . The K_D values for PI5P4K γ binding were determined by the commercially available KdELECT® and a respective protocol is available from DiscoverX.

Cell Culture. HEK 293T cells were cultured as recommended by ATCC. The cells were kept frozen, so only freshly thawed cells at early passage were used. Cells were maintained in DMEM media, which was supplemented with 10% FBS and 100 μ L/mL penicillin-streptomycin and incubated at 37 °C and 5% CO₂. No authentication was done by the authors.

Compounds and Reagents. Antibodies purchased from Cell Signaling Technology (Hanover, MA) were anti-PI5P4K α (5527) and anti-PI5P4K β (9694). Anti-GAPDH (MAB374) was obtained from EMD Millipore Corporation (Merck KGaA, Darmstadt, Germany).

Cellular Thermal Shift Assay (CETSA). Obtaining of the melting curves, as well as performing of the isothermal CETSA experiments and Western blot analysis were reported previously.¹⁷

Kinetic Solubility Assay. Solubility of selected compounds were determined according to methods as previously published.³⁹

Rat Liver Microsome Stability Assay. Single time point microsomal stability was determined in a 96-well HTS format. Sample preparation was automated using Tecan EVO 200 robot. High Resolution LC-MS (Thermo ZExactive) instrument was used to measure the percentage of compound remaining

after incubation using a previously described method.⁴⁰ Six standard controls were tested in each run: buspirone and propranolol (for short half-life), loperamide and diclofenac (for short to medium half-life), and carbamazepine and antipyrine (for long half-life). Briefly, the incubation consisted of 0.5 mg/mL microsomal protein, 1.0 μ M drug concentration, and NADPH regeneration system (containing 0.650 mM NADP⁺, 1.65 mM glucose 6-phosphate, 1.65 mM MgCl₂, and 0.2 unit/mL G6PDH) in 100 mM phosphate buffer at pH 7.4. The incubation was carried out at 37 °C for 15 min. The reaction was quenched by adding 555 μ L of acetonitrile (~1:2 ratio) containing 0.28 μ M albendazole (internal standard). Sample acquisition and data analysis was done using a previously described method.⁴⁰

Parallel Artificial Membrane Permeability Assay (PAMPA). Compound permeability was determined as previously described.⁴¹

ASSOCIATED CONTENT

Supporting Information

SMILES molecular formula strings (CSV)
Additional Tables, Figures, and Spectra (PDF)

AUTHOR INFORMATION

Corresponding Author

*(N.S.G.) E-mail: Nathanael_gray@dfci.harvard.edu

Author Contributions

T.D.M., S.C.S., T.Z., F.M.F., and N.S.G. conceived the project and designed the research strategy. S.C.S. performed the library screening and helped with planning experimental strategies. T.D.M., F.M.F., and T.Z. designed the compounds. C.V.M. synthesized the initial hit compound. T.D.M. synthesized the compounds presented. H.-S.S. and S.D.-P. generated the co-crystal structure. A.Y. and A.S. performed the biological evaluation of the compounds under supervision of M.D.H. and M.S.. J.D.C. and S.B.F. performed mass spectrometry analysis under supervision of J.A.M.. T.D.M. planned and performed the cellular assays. H.S. and L.C.C. were involved in the planning and provided expertise and feedback for the project. The manuscript was written by T.D.M. and the contributions of all authors. All authors have given approval of the final version of the manuscript. N.S.G. supervised the research.

Notes

The authors declare the following competing financial interest(s): N.S.G. is a founder, SAB member, and equity holder in Gatekeeper, Syros, Petra, C4, B2S, and Soltego. The Gray lab receives or has received research funding from Novartis, Takeda, Astellas, Taiho, Janssen, Kinogen, Voronoi, Her2llc, Deerfield, and Sanofi. L.C.C. is a founder and member of the Board of Directors (BOD) of Agios Pharmaceuticals and is a founder and receives research support from Petra Pharmaceuticals. These companies are developing novel therapies for cancer. J.A.M. serves on the SAB of 908 Devices. S.D.P. receives research support from Taiho Pharmaceuticals.

ACKNOWLEDGEMENTS

The authors would like to thank M. Kostic for her help and expertise with writing the manuscript.

Funding Sources

The authors would like to thank the National Institutes of Health for their generous financial support through grants R01 CA197329 (to N.S.G., subcontracted to S.D.P.), R01 NS089815 and R03 CA250020 (to J.A.M.), as well as R35 CA197588, R01 GM041890, and U54 CA210184 (to L.C.C.). This work was further supported by the Breast Cancer Research Foundation (to L.C.C.) and the NIH intramural research program (NCATS).

ABBREVIATIONS

ACVR2A, activin A receptor type 2A; ACVR2B, activin A receptor type 2B; ATCC, American type culture collection; BMPRI1, bone morphogenetic protein receptor type 1B; calc, calculated; CETSA, cellular thermal shift assay; CHAPS, 3-((3-cholamidopropyl) dimethylammonio)-1-propanesulfonate; CV, coefficient of variation; DMEM, Dulbecco's modified eagle medium; DPPS, 1,2-dipalmitoyl-*sn*-glycero-3-phosphoserine, sodium salt; EGTA, ethylene glycol-bis(β -aminoethyl ether)-*N,N,N',N'*-tetraacetic acid; FBS, fetal bovine serum; Hepes, 4-(2-hydroxyethyl)-1-piperazineethanesulfonic acid; MEK3, mitogen-activated protein kinase kinase 3; NCATS, national center for advancing translational studies; NIH, national institutes of health; PAINS, pan-assay interference compounds; PAMPA, parallel artificial membrane permeability assay; Pd₂(dba)₃, tris(dibenzylideneacetone)dipalladium(0); PI-4,5-P₂, phosphatidylinositol-4,5-bisphosphate; PI5P, phosphatidylinositol-5-phosphate; PI5P4K, phosphatidylinositol 5-phosphate 4-kinases; PI4P5K, phosphatidylinositol-4-phosphate 5-kinase; S₃₅, selectivity score for hits with percent control < 35; RLU, relative light units; SD, standard deviation; TGF β , transforming growth factor beta; TGFBR2, transforming growth factor beta receptor 2; UPLC, ultra-high pressure liquid chromatography; X-Phos, 2-dicyclohexylphosphino-2',4',6'-triisopropylphenyl.

PDB code for PI5P4K α with bound CVM-05-002 is 6UX9. Authors will release the atomic coordinates and experimental data upon article publication.

REFERENCES

- Rameh, L. E.; Toliás, K. F.; Duckworth, B. C.; Cantley, L. C. A new pathway for synthesis for phosphatidylinositol-4,5-bisphosphate. *Nature* 1997, 390 (6656), 192-196.
- Hu, A.; Zhao, X.-T.; Fu, T.; Wang, Y.; Liu, Y.; Shi, X.-J.; Luo, J.; Song, B.-L. PIP4K2A regulates intracellular cholesterol transport through modulating PI(4,5)₂ homeostasis. *J. Lipid Res.* 2018, 59, 507-514.
- Lamia, K. A.; Peroni, O. D.; Kim, Y.-B.; Rameh, L. E.; Kahn, B. B.; Cantley, L. C. Increased insulin sensitivity and reduced adiposity in phosphatidylinositol 5-phosphate 4-kinase $\beta^{-/-}$ mice. *Mol. Cell. Biol.* 2004, 24 (11), 5080-5087.
- Shim, H.; Wu, C.; Ramsamooj, S.; Bosch, K. N.; Chen, Z.; Emerling, B. M.; Yun, J.; Liu, H.; Choo-Wing, R.; Yang, Z.; Wulf, G. M.; Kuchroo, V. K.; Cantley, L. C. Deletion of the gene *Pip4k2c*, a novel phosphatidylinositol kinase, results in hyperactivation of the immune system. *PNAS* 2016, 113 (27), 7596-7601.
- Lundquist, M. R.; Goncalves, M. D.; Loughran, R. M.; Possik, E.; Vijayaraghavan, T.; Yang, A.; Pauli, C.; Ravi, A.; Verma, A.; Yang, Z.; Johnson, J. L.; Wong, J. C. Y.; Ma, Y.; Hwang, K. S.-K.; Weinkove, D.; Divecha, N.; Asara, J. M.; Elemento, O.; Rubin, M. A.; Kimmelman, A. C.; Ause, A.; Cantley, L. C. Emerling, B. M.

Phosphatidylinositol-5-phosphate 4-kinases regulate cellular lipid metabolism by facilitating autophagy. *Molecular Cell* 2017, 70 (3), 531-543.

- Bulley, S. J.; Droubi, A.; Clarke, J. H.; Anderson, K. E.; Stephens, L. R.; Hawkins, P. T.; Irvine, R. F. In B cells, phosphatidylinositol 5-phosphate 4-kinase- α synthesizes PI(4,5)P₂ to impact mTORC2 and Akt signaling. *PNAS* 2016, 113 (38), 10571-10576.
- Keune, W.-J.; Jones, D. R.; Divecha, N. PtdIns5P and Pin1 in oxidative stress signaling. *Advances in Biological Regulation* 2013, 53 (2), 179-189.
- Al-Ramahi, I.; Giridharan, S. S. P.; Chen, Y.-C.; Patnaik, S.; Safren, N.; Hasegawa, J.; de Haro, M.; Wagner Gee, A. K.; Titus, S. A.; Jeong, H.; Clarke, J.; Krainc, D.; Zheng, W.; Irvine, R. F.; Barmada, S.; Ferrer, M.; Southall, N.; Weisman, L. S.; Botas, J.; Marugan, J. J. Inhibition of PIP4Ky ameliorates the pathological effects of mutant huntingtin protein. *eLife* 2017, e29123; DOI: 10.7554/eLife.29123.
- Jude, J. G.; Spencer, G. J.; Somerville, T. D. D.; Jones, D. R.; Divecha, N.; Somerville, T. C. P. A targeted knockdown screen of genes coding for phosphoinositide modulators identifies *PIP4K2A* as required for acute myeloid leukemia cell proliferation and survival. *Oncogene* 2015, 34 (10), 1253-1262.
- Luoh, S.-W.; Venkatesan, N.; Tripathi, R. Overexpression of the amplified *Pip4k2 β* gene from 17q11-12 in breast cancer cells confers proliferation advantage. *Oncogene* 2004, 23, 1354-1363.
- Emerling, B. M.; Hurov, J. B.; Poulogiannis, G.; Tsukazawa, K. S.; Choo-Wing, R.; Wulf, G. M.; Bell, E. L.; Shim, H.-S.; Lamia, K. A.; Rameh, L. E.; Bellinger, G.; Sasaki, A. T.; Asara, J. M.; Yuan, X.; Bullock, A.; DeNicola, G. M.; Song, J.; Brown, V.; Signoretti, S.; Cantley, L. C. Depletion of a putatively druggable class of phosphatidylinositol kinases inhibits growth of p53-null tumors. *Cell* 2013, 155 (4), 844-857.
- Davis, M. I.; Sasaki, A. T.; Shen, M.; Emerling, B. M.; Thorne, N.; Michael, S.; Pragani, R.; Boxer, M.; Sumita, K.; Takeuchi, K.; Auld, D. S.; Li, Z.; Cantley, L. C.; Simeonov, A. A Homogeneous, high-throughput assay for phosphatidylinositol 5-phosphate 4-kinase with a novel, rapid substrate preparation. *PLoS ONE* 2013, 8 (1), e54127; DOI: 10.1371/journal.pone.0054127.
- Kitagawa, M.; Liao, P.-J.; Lee, K. H.; Wong, J.; Shang, S. C.; Minami, N.; Sampetean, O.; Saya, H.; Lingyun, D.; Prabhu, N.; Diam, G. K.; Sobata, R.; Larsson, A.; Nordlung, P.; McCormick, F.; Ghosh, S.; Estein, D. M.; Dymock, B. W.; Lee, S. H. Dual blockade of the lipid kinase PIP4Ks and mitotic pathways lead to cancer-selective lethality. *Nat. Com.* 2017, 8 (1), 1-13.
- Voss, M. D.; Czechtizky, W.; Li, Z.; Rudolph, C.; Petry, S.; Brummerhop, H.; Langer, T.; Schiffer, A.; Schaefer, H.-L.; Discovery and pharmacological characterization of a novel small molecule inhibitor of phosphatidylinositol-5-phosphate 4-kinase, type II, beta. *Biochemical and Biophysical Research Communications* 2014, 449 (3), 327-331.
- Clarke, J. H.; Giudici, M.-L.; Burke, J. E.; Williams, R. L.; Maloney, D. J.; Marugan, J.; Irvine, R. F. The function of phosphatidylinositol 5-phosphate 4-kinase γ (PI5P4Ky) explored using a specific inhibitor that targets the PI5P-binding site. *Biochem. J.* 2015, 466 (2), 359-367.
- Sivakumaren, S. C.; Shim, H.; Zhang, T.; Ferguson, F. M.; Lundquist, M. R.; Browne, C. M.; Seo, H.-S.; Paddock, M. N.; Manz, T. D.; Jiang, B.; Hao, M.-F.; Krishnan, P.; Wang, D. G.; Yang, J.; Kwiatkowski, N. P.; Ficarro, S. B.; Cunningham, J. M.; Marto, J. A.; Dhe-Paganon, S.; Cantley, L. C.; Gray, N. S. Targeting the PI5P4K lipid kinase family in cancer using novel covalent inhibitors. *Cell Chem Biol.* 2020; DOI: 10.1016/j.chembiol.2020.02.003.
- Manz, T. D.; Sivakumaren, S. C.; Yasgar, A.; Hall, M. D.; Davis, M. I.; Seo, H.-S.; Card, J. D.; Shim, H.; Ficarro, S. B.; Dhe-Paganon, S.; Sasaki, A. T.; Boxer, M. B.; Simeonov, A.; Cantley, L. C.; Shen, M.; Zhang, T.; Ferguson, F. M.; Gray, N. S. Structure-activity relationship study of covalent pan-phosphatidylinositol 5-phosphate 4-kinase inhibitors. *ACS Med. Chem. Lett.* 2019, 11 (3), 346-352.
- Thress, K. S.; Pawletz, C. P.; Felip, E.; Cho, B. C.; Stetson, D.; Dougherty, B.; Lai, Z.; Markovets, A.; Vivancos, A.; Kuang, Y.; Ercan, D.; Matthews, S.; Cantarini, M.; Barrett, J. C.; Jänne, P. A.; Oxnard, G. R. Acquired *EGFR C797S* mediates resistance to AZD9291

in advanced non-small cell lung cancer harboring *EGFR* T790M. *Nat Med.* 2015, *21* (6), 560-562.

(19) Kenny, P. W. Comment on the ecstasy and agony of assay interference compounds. *J. Chem. Inf. Model.* 2017, *57* (3), 387-390.

(20) Baell, J. B.; Holloway, G. A. New substructure filters for removal of pan assay interference compounds (PAINS) from screening libraries and for their exclusion in bioassays. *J. Med. Chem.* 2010, *53*, 2719-2740.

(21) Baell, J. B.; Nissink, J. W. M. Seven year itch: Pan-assay interference compounds (PAINS) in 2017 – utility and limitations. *ACS Chem Biol.* 2018, *13*, 36-44.

(22) Mendgen, T.; Steuer, C.; Klein, C. D. Privileged scaffolds or promiscuous binders: A comparative study on rhodanines and related heterocycles in medicinal chemistry. *J. Med. Chem.* 2012, *55*, 743-753.

(23) Camps, M.; Rueckle, T.; Ji, H.; Ardisson, V.; Rintelen, F.; Shaw, J.; Ferrandi, C.; Chabert, C.; Gillieron, C.; Francon, B.; Martin, T.; Gretener, D.; Perrin, D.; Leroy, D.; Vitte, P.-A.; Hirsch, E.; Wyman, M. P.; Cirillo, R.; Schwarz, M. K.; Rommel, C. Blockade of PI3K γ suppresses joint inflammation and damage in mouse models of rheumatoid arthritis. *Nat Med.* 2005, *11* (9), 936-943.

(24) Ye, X.; Zhou, W.; Li, Y.; Sun, Y.; Zhang, Y.; Ji, H.; Lai, Y. Darbufelone, a novel anti-inflammatory drug, induces growth inhibition of lung cancer cells both in vitro and in vivo. *Cancer Chemother Pharmacol.* 2010, *66*, 277-285.

(25) Ghatak, S.; Vyas, A.; Misra, S.; O'Brien, P.; Zambre, A.; Fresco, V. M.; Markwald, R. R.; Swamy, K. V.; Afrasiabi, Z.; Choudhury, A.; Khetmalas, M.; Padhye, S. Novel di-tertiary-butyl phenylhydrazones as dual cyclooxygenase-2/5-lipoxygenase inhibitors: Synthesis, COX/LOX inhibition, molecular modeling, and insights into their cytotoxicities. *J. Bioorg. Med. Chem. Lett.* 2014, *24*, 317-324.

(26) Dakin, L. A.; Block, M. H.; Chen, H.; Code, E.; Dowling, J. E.; Feng, X.; Ferguson, A. D.; Green, I.; Hird, A. W.; Howard, T.; Keeton, E. K.; Lamb, M. L.; Lyne, P. D.; Pollard, H.; Read, J.; Wu, A. J.; Zhang, T.; Zheng, X. Discovery of novel benzylidene-1,3-thiazolidine-2,4-diones as potent and selective inhibitors of the PIM-1, PIM-2, and PIM-3 protein kinases. *J. Bioorg. Med. Chem. Lett.* 2012, *22*, 4599-4604.

(27) Cortes, J.; Tamura, K.; DeAngelo, D. J.; de Bono, J.; Lorente, D.; Minden, M.; Uy, G. L.; Kantarjian, H.; Chen, L. S.; Gandhi, V.; Godin, R.; Keating, K.; McEachern, K.; Vishwanathan, K.; Pease, J. E.; Dean, E. Phase I studies of AZD1208, a proviral integration Moloney virus kinase inhibitor in solid and hematological cancers. *British Journal of Cancer* 2018, *118*, 1425-1433.

(28) Mathre, S.; Reddy, K. B.; Ramya, V.; Krishnan, H.; Ghosh, A.; Raghu, P. Functional analysis of the biochemical activity of mammalian phosphatidylinositol 5 phosphate 4-kinase enzymes. *Biosci Rep.* 2019, *39* (2); DOI: 10.1042/BSR20182210.

(29) Clarke, J. H.; Emson, P.C.; Irvine, R. F. Localization of phosphatidylinositol phosphate kinase II gamma in kidney to a membrane trafficking compartment within specialized cells of the nephron. *Am J Physiol Renal Physiol.* 2008, *295* (5), F1422-F1430.

(30) Zhang, J.; Yang, P. L.; Gray, N. S. Targeting cancer with small molecule kinase inhibitors. *Nat Rev Cancer.* 2009, *9* (1), 28-39.

(31) Roskoski, R. Jr. Classification of small molecule protein kinase inhibitors based upon the structures of their drug-enzyme complexes. *Pharmacol Res.* 2016, *103*, 26-48.

(32) Zhao, Z.; Wu, H.; Wang, L.; Liu, Y.; Knapp, S.; Liu, Q.; Gray, N. S. Exploration of type II binding mode: A privileged approach for kinase inhibitor focused drug discovery? *ACS Chem Biol.* 2014, *9* (6), 1230-1241.

(33) Massague, J.; Gomis, R. R. The logic of TGF β signaling. *FEBS Lett.* 2006, *580* (12), 2811-2820.

(34) Chung, H.; Young, D. J.; Lopez, C. G.; Le, T.-A. T.; Lee, J. K.; Ream-Robinson, D.; Huang, S. C.; Carethers, J. M. Mutation rates of *TGFBR2* and *ACVR2* coding microsatellites in human cells with defective DNA mismatch repair. 2008, *3* (10), e3463; DOI: 10.1371/journal.pone.0003463.

(35) Jung, B. H.; Beck, S. E.; Cabral, J.; Chau, E.; Cabrera, B. L.; Fiorino, A.; Smith, E. J.; Bocanegra, M.; Carethers, J. M. *Activin type 2 receptor* restoration in MSI-H colon cancer suppresses growth and enhances migration with activin. *Gastroenterology.* 2007, *132* (2), 633-644.

(36) Henderson, M. J.; Holbert, M. A.; Simeonov, A.; Kallal, L. A. High-throughput cellular thermal shift assays in research and drug discovery. *SLAS Discov.* 2020, *25* (2), 137-147.

(37) Bulley, S. J.; Clarke, J. H.; Droubi, A.; Giudici, M.-L.; Irvine, R. F. Exploring phosphatidylinositol 5-phosphate 4-kinase function. *Adv Biol Regul.* 2015, *57*, 193-202.

(38) Marty, M. T.; Baldwin, A. J.; Marklund, E. G.; Hochberg, G. K. A.; Benesch, J. L. P.; Robinson, C. V. Bayesian deconvolution of mass and ion mobility spectra: From binary interactions to polydisperse ensembles. *Anal Chem.* 2015, *87* (8), 4370-4376.

(39) Sun, H.; Shah, P.; Nguyen, K.; Yu, K. R.; Kerns, E.; Kabir, M.; Wang, Y.; Xu, X. Predictive models of aqueous solubility of organic compounds built on a large dataset of high integrity. *Bioorg Med Chem.* 2019, *27* (14), 3110-3114.

(40) Shah, P.; Kerns, E.; Nguyen, D.-T.; Obach, S.; Wang, A. Q.; Zakharov, A.; McKew, J.; Simeonov, A.; Hop, C. E. C. A.; Xu, X. An automated high-throughput metabolic stability assay using an integrated high-resolution accurate mass method and automated data analysis software. *Drug Metab Dispos.* 2016, *44* (10), 1653-1661.

(41) Sun, H.; Nguyen, K.; Kerns, E.; Yan, Z.; Yu, K. R.; Shah, P.; Jadhav, A.; Xu, X. Highly predictive and interpretable models for PAMPA permeability. *Bioorg Med Chem.* 2017, *25* (3), 1266-1276.

Table of Contents Graphic

